Measurement of TEER—Barrier integrity in *in vitro* BBB models was analyzed by measurement of TEER. TEER was measured using an epithelial-volt-ohm meter and Endohm-24 chamber electrodes (World Precision Instruments). TEER of coated but cell-free filters was subtracted from the measured TEERs of models shown as $\Omega \times cm^2$.

Real-time PCR Analysis—The mRNA levels of TJ proteins were evaluated by real-time PCR analysis. Total RNA was extracted using a CellAmp™ Direct RNA Prep kit (Takara Bio Inc., Shiga, Japan) and reverse-transcribed with oligo(dT) and random primers using a PrimeScript RT reagent kit (Takara Bio Inc.). Relative real-time PCR was carried out using SYBR Premix Ex Taq™ II (Takara Bio Inc.) and Thermal Cycler Dice Real-time system TP-800 (Takara Bio Inc.) in accordance with the manufacturer's protocols. The oligonucleotide sequences used for the primer sets were 5′-GCTTATCTTGGGAGCCTGGACA-3′ and 5′-GTCATTGCTTGGTGCATAATGATTG-3′ for occludin, 5′-CACCACTACCAGCAGTCGATAA-3′ and 5′-GTGTCGTCTGTCACCATCTGGAA-3′ for claudin 3, 5′-AGTTAAGGCACGGGTAGCACTCAC-3′ and 5′-CAACGATGTTGGCGAACCAG-3′ for claudin 5, and 5′-GCCAATCACAATTGCGAAGATG-3′ and 5′-GCCACTCGAGCTGATCTGTCAC-3′ for apoE.

Western Blotting—The protein expression levels of occludin, PKCη, and phosphorylated PKCη in *in vitro* BBB models were determined by Western blotting. Cells were washed with PBS three times, harvested using a cell scraper, and lysed by sonication in radioimmuneprecipitation assay buffer (1% Nonidet P-40, 0.5% sodium deoxycholate, 0.1% SDS, 150 mM NaCl, 50 mM Tris-HCl (pH 8.0), 1 mM EDTA). Cell lysates were subjected to SDS-PAGE with 7.5% gels (WAKO Pure Chemicals, Osaka, Japan) and transferred to polyvinylidene difluoride membranes (Millipore). The membrane was blotted with a primary antibody followed by a horseradish peroxidase-labeled secondary antibody (Cell Signaling Technology, Inc., Beverly, MA). The blot was developed using chemiluminescent substrate ECL Plus (GE Healthcare). Signals were visualized and quantified using a LAS-3000 miniluminescent image analyzer (Fujifilm, Tokyo, Japan). The protein level in cell lysates was normalized to the expression level of the actin protein. The phosphorylation state of occludin was analyzed by immunoprecipitation. For immunoprecipitation, cell lysates were incubated with magnetic protein G beads (Dynal, Hamburg, Germany) linked with an anti-Thr(P) or anti-Tyr(P) antibody. The obtained precipitates were washed three times with PBS and incubated at 70 °C for 10 min in SDS sample buffer. Dissociated occludin in the supernatant was analyzed by Western blotting as described above.

Statistical Analyses—The collected data were analyzed by one-way analysis of variance (ANOVA) including appropriate variables followed by Dunnett's test or unpaired Student's *t* test (comparison between two groups). Results were considered significant when $p < 0.05$.

RESULTS

BBB Integrity Was Impaired in ApoE4-BBB Model—First, we examined whether mBECs and primary pericytes express apoE. We confirmed that the mRNA level of apoE in mBECs was about 1,000 times lower than that in primary astrocytes (data not shown), and we did not detect apoE in the culture media of mBECs and primary pericytes by Western blotting (data not shown). Thus, we prepared mBECs and primary pericytes from wild-type mice and astrocytes from apoE3- or apoE4-knock-in mice, WT mice, and apoE-KO mice for the preparation of an *in vitro* BBB model. TEER increased in a manner that depended on the number of days of culture after preparing the *in vitro* BBB model and was significantly lower in the apoE4-BBB model than in the apoE3-BBB model on days 5 and 7 (Fig. 1*A*). We also evaluated TEER in *in vitro* BBB models with astrocytes prepared from WT mice, expressing endogenous mouse apoE, and astrocytes prepared from apoE-KO mice. We found that TEER

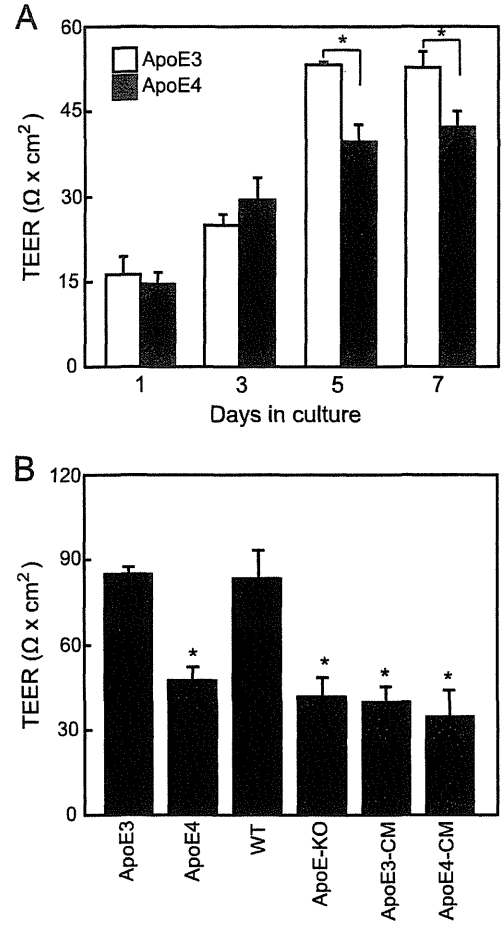

FIGURE 1. **TEER in apoE3-BBB, apoE4-BBB, WT-BBB, and apoE-KO-BBB models.** *A*, triple co-culture BBB models were prepared by using primary pericytes and mBECs from WT mouse brains and primary astrocytes from human apoE3- or apoE4-knock-in mice and were cultured for 7 days. TEER was measured on the indicated culture days and presented as $\Omega \times cm^2$. The data presented are means ± S.D. (*error bars*) ($n = 3$). *, $p < 0.001$ compared with the values of apoE3-BBB models on day 7 or day 5 (unpaired Student's *t* test). *B*, triple co-culture BBB models were prepared by using primary pericytes and mBECs from WT mouse brains and primary astrocytes from human apoE3- or apoE4-knock-in mice, WT mice, or apoE-KO mice and were cultured for 7 days. To determine the effect of the apoE-containing conditioned media, double co-culture model using primary pericytes and mBECs in the absence of astrocytes was sued. The conditioned media (48 h) from apoE3-expressing astrocytes (apoE3-CM) or apoE4-expressing astrocytes (apoE4-CM) were added only to the luminal side of double co-culture models and maintained for 7 days. Then, TEER was measured, and the values are presented as $\Omega \times cm^2$. The data presented are means ± S.D. ($n = 3$). *, $p < 0.05$ *versus* apoE3-BBB model.

in the WT-BBB model was comparable with that in the apoE3-BBB model, whereas TEER in the apoE-KO-BBB model was significantly lower than that in the apoE3-BBB model (Fig. 1*B*). Furthermore, we performed experiments to determine the effect of apoE-containing media on BBB integrity. The conditioned media of primary astrocytes expressing apoE3 (apoE3-CM) or apoE4 (apoE4-CM) were added to the luminal side of the co-culture model with pericytes and mBECs in the absence of astrocytes. TEER was significantly lower in these models than in the apoE3-BBB model (Fig. 1*B*).

ApoE Isoforms Do Not Affect Expression Levels of TJ Proteins—Next, we analyzed the expression levels of occludin, claudin 3, and claudin 5, all of which were reported to be major constituents of TJ strands (15). Each BBB model was cultured for 7 days, and the mRNA levels of these proteins in mBECs were analyzed by real-time PCR. Results are shown as relative ratios to actin. The expression levels of occludin (Fig. 2*A*), claudin 3, and claudin 5 (data not shown) in the apoE3-BBB model were comparable with those in the apoE4-BBB, WT-BBB, and apoE-KO-BBB models.

Thr Phosphorylation of Occludin Was Regulated in an ApoE Isoform-dependent Manner—The phosphorylation of occludin at Tyr residues is reported to negatively regulate TJ integrity (26) whereas phosphorylation at Thr residues is required for the assembly of occludin into TJs (19). We then determined whether the phosphorylation of occludin is regulated in an apoE isoform-dependent manner. On day 7, mBECs were harvested using a cell scraper, and the level of phosphorylated occludin was determined by immunoprecipitation followed by Western blotting. We did not detect the phosphorylation of occludin at Tyr residues (data not shown). The levels of phosphorylated occludin at Thr residues were significantly lower in the apoE4-BBB model than in the apoE3-BBB model (Fig. 2*B*). The phosphorylated occludin at Thr residues was abolished in the apoE-KO-BBB model, whereas the level of phosphorylated occludin in the WT-BBB model was similar to that in the apoE3-BBB model (Fig. 2*B*). Consistent with the results of real-time PCR analysis, the protein level of occludin in the apoE3-BBB model was comparable with those in the apoE4-BBB, WT-BBB, and apoE-KO-BBB models (Fig. 2*B*). Recently, it has been reported that PKCη regulates the phosphorylation of occludin at Thr residues in epithelial TJs (19). We then analyzed the activation states of PKCη in the *in vitro* BBB models. On day 7, mBECs in the BBB models were harvested, lysed, and subjected to SDS-PAGE followed by immunoblotting with the antibody specific for phosphorylated PKCη at the Ser-674 residue, which is an activated form of PKCη (27). As shown in Fig. 2*C*, phosphorylation of PKCη was significantly attenuated in the apoE4-BBB model compared with the apoE3-BBB model, indicating that apoE isoforms differentially influence the activation of PKCη. The level of phosphorylated PKCη was significantly lower in the apoE-KO-BBB model than in the apoE3-BBB model, and the level of phosphorylated PKCη in the WT-BBB model was comparable with that in the apoE3-BBB model (Fig. 2*C*). We examined the phosphorylation of other PKC isoforms, PKCι and PKCζ, which interact directly with TJs (17), and found no significant difference in the levels of phosphorylated PKC isoforms (data not shown).

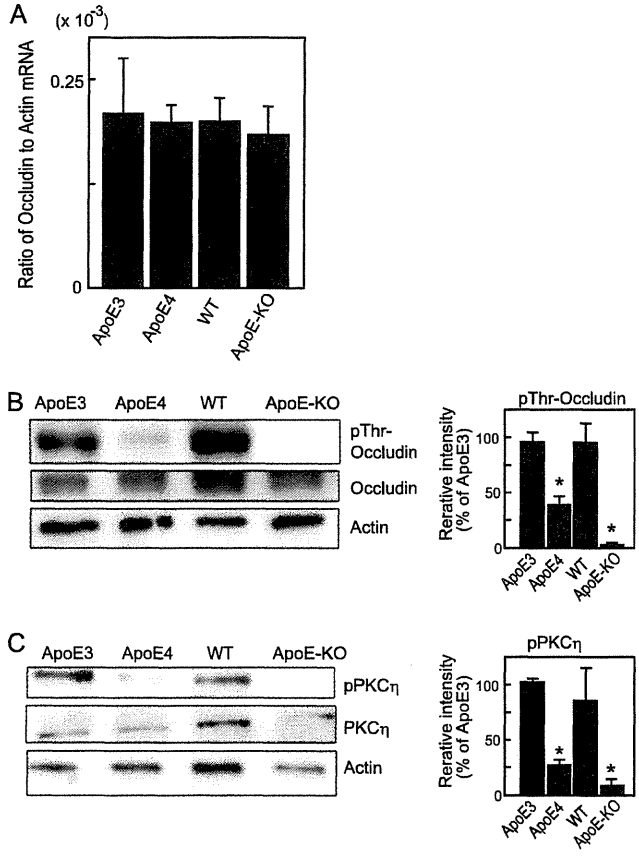

FIGURE 2. **Phosphorylation of occludin and PKCη in mBECs of apoE3-BBB, apoE4-BBB, WT-BBB, and apoE-KO-BBB models.** *A*, triple co-culture BBB models were prepared by using primary pericytes and mBECs from WT mouse brains and primary astrocytes from human apoE3 or apoE4 knock-in mice, WT mice, or apoE-KO mice and were cultured for 7 days. Total RNA of mBECs was collected. Relative real-time PCR analysis was performed to compare the expression levels of occludin. Results are shown as relative ratios to actin. The data presented are means ± S.D. (*error bars*) ($n = 3$). *B*, triple co-cultured models were cultured for 7 days. On day 7, mBECs were harvested, and the obtained cell lysates were subjected to immunoprecipitation and Western blotting. For the detection of occludin phosphorylated at its Thr residues, immunoprecipitation with the anti-Thr(P) antibody followed by immunoblotting with the anti-occludin antibody was performed. For the detection of total occludin, cell lysates were subjected to SDS-PAGE followed by probing with the anti-occludin antibody. The anti-β actin antibody was used as the loading control. The graph shows the levels of phosphorylated occludin at Thr residues and total occludin. The data presented are means ± S.D. ($n = 3$). *, $p < 0.001$ *versus* apoE3-BBB model. *C*, triple co-cultured models were cultured for 7 days. On day 7, mBECs were harvested, and the obtained cell lysates were subjected to Western blotting with the anti-phosphorylated PKCη and anti-PKCη antibodies. The graph shows the levels of phosphorylated and total pPKCη. The data presented are means ± S.D. ($n = 3$). *, $p < 0.001$ *versus* apoE3-BBB model.

LRP1 Is Involved in the Regulation of the TJ Integrity in the ApoE3-BBB Model—ApoE is a ligand for receptors of the LDL receptor (LDLR) superfamily, several of which act both as endocytic receptors (28) and signaling receptors (5). Thus, we examined the effect of the RAP on the phosphorylation of PKCη. RAP, a 39-kDa protein, is a specialized chaperone of members of the LDLR family, including LRP1 (29, 30). RAP binds to LRP1 at multiple sites (29, 30) with high affinity (K_D = 1–10 nM) (31). RAP has also been used extensively as an antagonist of LRP1 (32). On day 7, RAP (1 μM) was added to the media of astrocytes in an *in vitro* BBB model and cultured for 4 h at 37 °C. After

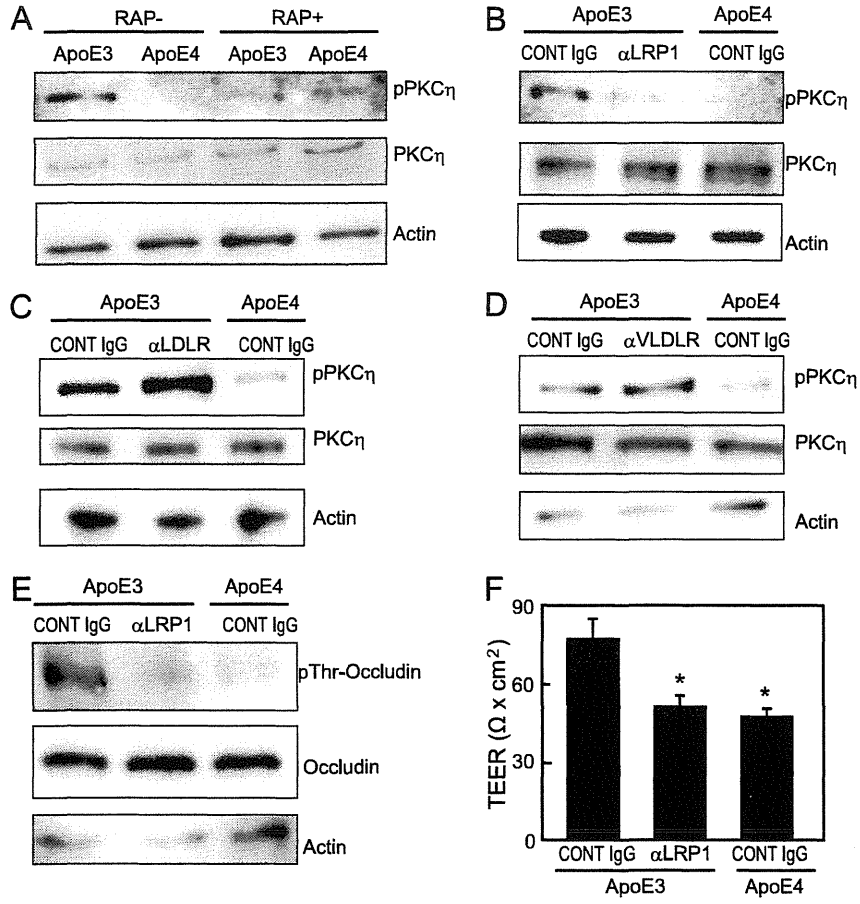

FIGURE 3. **LRP1 is involved in the regulation of TJ integrity in the apoE3-BBB model.** *A–D*, apoE3- and apoE4-BBB models were cultured for 7 days. On day 7, the *in vitro* BBB models were treated with RAP (*A*) (1 μM) or the anti-LRP1 (*B*), anti-LDLR (*C*), or anti-VLDLR antibody (*D*) (25 μg/ml) for 4 h at 37 °C. After treatment, mBECs were harvested using a cell scraper, and the obtained cell lysates were subjected to Western blotting using anti-phosphorylated PKCη and anti-PKCη antibodies. *E*, apoE3- and apoE4-BBB models were cultured for 7 days. On day 7, the *in vitro* BBB models were treated with the anti-LRP1 antibody or isotype IgG (25 μg/ml) for 4 h at 37 °C. After treatment, mBEC lysates were immunoprecipitated with the polyclonal anti-Thr(P) antibody, and the immunoprecipitates were subjected to Western blotting using the anti-occludin antibody or anti-phosphooccludin antibody. *F*, apoE3- and apoE4-BBB models were cultured for 7 days and then treated with the anti-LRP1 antibody or isotype IgG (25 μg/ml) for 4 h at 37 °C. After treatment, TEER was measured, and the values are presented as $\Omega \times cm^2$. The data presented are means ± S.D. (*error bars*) ($n = 3$). *, $p < 0.005$ compared with the values of apoE3-BBB models treated with control IgG (Dunnett's test).

incubation, the phosphorylation of PKCη in mBECs was analyzed by Western blotting. The treatment of the apoE3-BBB model with RAP attenuated the phosphorylation of PKCη to a level similar to that of the apoE4-BBB model (Fig. 3*A*). Because RAP inhibits LRP1 as well as the LDLR (29) and because apoE-containing particles can bind to the very low-density lipoprotein (VLDL) receptor (33), we next treated the apoE3-BBB model with the anti-LRP1, anti-LDLR, or anti-VLDLR antibody (25 μg/ml), which recognizes the extracellular domain of LRP1, LDLR, or VLDLR, respectively, on day 7 for 4 h at 37 °C to determine whether specific apoE receptors are involved in PKCη phosphorylation. Among these antibodies, only the anti-LRP1 receptor antibody suppressed the phosphorylation of PKCη (Fig. 3, *B–D*). Consistent with this suppression of PKCη phosphorylation, the treatment of the apoE3-BBB model with the anti-LRP1 antibody also suppressed the phosphorylation of occludin at Thr residues (Fig. 3*E*). Next, we examined whether treatment of the apoE3-BBB model with the anti-LRP1 antibody impairs TJ integrity. The prepared apoE3-BBB model was cultured for 7 days, and the anti-LRP1 antibody (25 μg/ml) was added to the astrocyte culture medium. After further incubation of the cultures for 4 h at 37 °C, TJ integrity was evaluated by measuring TEER. Treatment of the apoE3-BBB model with the anti-LRP1 antibody significantly decreased TEER (Fig. 3*F*), indicating that TJ integrity requires the function of apoE receptor LRP1.

BBB Integrity Is Impaired in ApoE4-knock-in Mice—Finally, we evaluated the BBB integrity in human apoE3-, apoE4-knock-in mice, and apoE-KO mice. BBB integrity was evaluated using an Evans blue dye technique. Consistent with the results shown in Fig. 1, BBB integrity was impaired in the apoE4-knock-in mice compared with the apoE3-knock-in mice (Fig. 4). Consistent with previous studies (9, 11), BBB integrity was impaired in the apoE-KO mice (Fig. 4). We found a higher amount of leakage in the cerebellum of human apoE-knock-in mice than in the cerebrum, which is consistent with the findings of previous studies using apoE-KO mice (9, 11).

DISCUSSION

In this report, we provided evidence that TEER is lower in the apoE4-BBB and apoE-KO models than in the apoE3-BBB and WT-BBB models. The activation of PKCη and the phosphory-

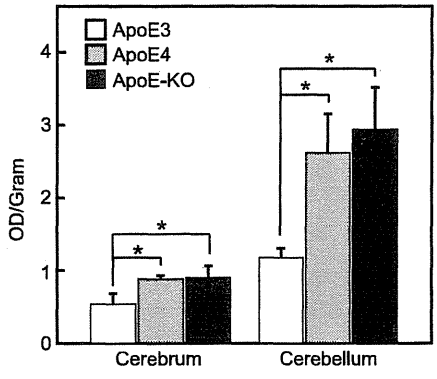

FIGURE 4. **BBB integrity is impaired in apoE4-knock-in mice.** The BBB integrity in apoE3-knock-in mice, apoE4-knock-in mice, and apoE-KO mice was evaluated using an Evans blue dye technique. Two hundred microliters of 20% mannitol was injected through the tail vein. Thirty minutes after injection, 200 μl of 2% Evans blue dye was injected intraperitoneally. The distribution of the dye was confirmed by a visible change in the color of the skin within 1 h after injection. Three hours after the injection, the mice were killed, and their brains were removed. The cerebrum and cerebellum were immediately collected, weighed, and incubated in 500 μl of formamide for 72 h at room temperature in the dark. The absorbance of the extracted dye was measured at 630 nm. The data presented are means ± S.D. (*error bars*) ($n = 3$). *, $p < 0.05$.

lation of occludin at its Thr residues, which regulates TJ integrity, were dependent on the apoE isoform. Furthermore, the treatment of the apoE3-BBB model with the anti-LRP1 antibody diminished the activation of PKCη and phosphorylation of occludin, suggesting that LRP1 may be involved in the regulation of TJ integrity through the activation of PKCη and phosphorylation of occludin at its Thr residues in the apoE3-BBB model. Our results also indicate that this pathway is impaired in the apoE4-BBB model. Consistent with the results of *in vitro* studies, BBB permeability was increased in the apoE4-knock-in mice and apoE-KO mice compared with the apoE3-knock-in mice. As revealed in previous studies (7, 8), astrocytes are involved in the control of BBB integrity. Astrocytes are considered to be the major source of apoE in the CNS (4–6), and apoE deficiency leads to BBB leakage (9–11). These lines of evidence suggest that astrocytes may regulate BBB integrity through apoE. In the present study, our findings indicate that apoE secreted from astrocytes is involved in the regulation of TJ integrity through the activation of PKCη and phosphorylation of occludin at its Thr residues in an LRP1-mediated manner in the apoE3-BBB model and that this pathway is impaired in the apoE4-BBB model. We provide the first evidence that TJ integrity in BBB is regulated in an apoE isoform-dependent manner.

ApoE-containing particles act as ligands of LDLR family members such as LRP1 and play critical roles in maintaining brain lipid homeostasis and associated synaptic and neuronal integrity (4, 34). Previous studies have shown that apoE induces lipid release to generate HDL-like particles from macrophages and astrocytes in an isoform-dependent manner; apoE3 induces a greater lipid release than apoE4 (35–39). In addition to functioning as lipid carriers, a recent study showed that apoE3-containing particles act as signaling molecules through LRP1 to activate PKCδ, a novel PKC isoform (40), and protect neurons from apoptosis in an apoE isoform-dependent manner (41). Here, we showed that apoE regulates the activation of PKCη, which is also a novel PKC isoform (40), through LRP1 in mBECs in the *in vitro* BBB model. Thus, our results suggest that apoE-containing particles also act as signaling molecules to regulate the activation of PKCη, the subsequent phosphorylation of occludin at its Thr residues, and TJ integrity. Our findings also indicate that apoE4-containing particles might be less efficient as signaling molecules than apoE3-containing particles.

ApoE4 is a major risk factor for AD. Although how apoE4 influences AD onset and progression has not been fully understood yet, recent studies suggest that the differential effects of apoE isoforms on amyloid-β (Aβ) aggregation and clearance could play important roles in AD pathogenesis. Human apoE-transgenic mice display an isoform-specific pattern of Aβ deposition (E3 < E4) (42–46). Previous studies have shown that lipid-poor apoE4 and lipid-free apoE4 enhance Aβ production by increasing LRP1- and apoER2-mediated endocytosis of an amyloid precursor protein (47, 48). ApoE also facilitates the proteolytic clearance of Aβ from the brain in an apoE isoform-dependent manner and requires its lipidation (49). Considering BBB as a pathway of Aβ clearance in the brain (50–52), a recent study has shown that Aβ complexed to apoE2 and apoE3 is cleared out of the brain at a significantly higher rate than Aβ complexed to apoE4 (53). Interestingly, several studies have demonstrated that there is an increased permeability in the BBB of the AD model mice compared with age-matched control mice (54, 55) and that Aβ fibrils could increase the permeability of bovine pulmonary arterial endothelial cells, as detected by TEER measurement (56). Furthermore, a recent study using pericyte-deficient mice has shown that BBB breakdown is associated with the accumulation of neurotoxic and/or vasculotoxic serum proteins in the brain, which leads to secondary neurodegenerative changes (57). In this study, we provide evidence that TJ integrity in BBB is impaired in the apoE4-BBB model and apoE4-knock-in mice. Thus, these lines of evidence suggest that apoE4 may affect AD pathogenesis and/or neurodegeneration through its effects on BBB. We have shown using *in vitro* and *in vivo* models that apoE regulates the activation of PKCη, the phosphorylation of occludin at Thr residues, and TJ integrity in an apoE isoform-dependent manner. Further study will be needed to elucidate the contribution of BBB impairment to AD pathogenesis.

REFERENCES

1. Mahley, R. W. (1988) *Science* **240,** 622–630
2. Corder, E. H., Saunders, A. M., Strittmatter, W. J., Schmechel, D. E., Gaskell, P. C., Small, G. W., Roses, A. D., Haines, J. L., and Pericak-Vance, M. A. (1993) *Science* **261,** 921–923
3. Saunders, A. M., Strittmatter, W. J., Schmechel, D., George-Hyslop, P. H., Pericak-Vance, M. A., Joo, S. H., Rosi, B. L., Gusella, J. F., Crapper-MacLachlan, D. R., Alberts, M. J., *et al.* (1993) *Neurology* **43,** 1467–1472
4. Bu, G. (2009) *Nat. Rev. Neurosci.* **10,** 333–344
5. Herz, J., and Bock, H. H. (2002) *Annu. Rev. Biochem.* **71,** 405–434
6. Herz, J., and Chen, Y. (2006) *Nat. Rev. Neurosci.* **7,** 850–859
7. Janzer, R. C., and Raff, M. C. (1987) *Nature* **325,** 253–257
8. Rubin, L. L., and Staddon, J. M. (1999) *Annu. Rev. Neurosci.* **22,** 11–28
9. Hafezi-Moghadam, A., Thomas, K. L., and Wagner, D. D. (2007) *Am. J. Physiol. Cell Physiol.* **292,** C1256–1262
10. Methia, N., André, P., Hafezi-Moghadam, A., Economopoulos, M., Thomas, K. L., and Wagner, D. D. (2001) *Mol. Med.* **7,** 810–815
11. Fullerton, S. M., Shirman, G. A., Strittmatter, W. J., and Matthew, W. D. (2001) *Exp. Neurol.* **169,** 13–22
12. Reese, T. S., and Karnovsky, M. J. (1967) *J. Cell Biol.* **34,** 207–217

13. Hori, S., Ohtsuki, S., Hosoya, K., Nakashima, E., and Terasaki, T. (2004) *J. Neurochem.* **89,** 503–513
14. Tao-Cheng, J. H., Nagy, Z., and Brightman, M. W. (1987) *J. Neurosci.* **7,** 3293–3299
15. Tsukita, S., and Furuse, M. (1999) *Trends Cell Biol.* **9,** 268–273
16. Basuroy, S., Sheth, P., Kuppuswamy, D., Balasubramanian, S., Ray, R. M., and Rao, R. K. (2003) *J. Biol. Chem.* **278,** 11916–11924
17. Helfrich, I., Schmitz, A., Zigrino, P., Michels, C., Haase, I., le Bivic, A., Leitges, M., and Niessen, C. M. (2007) *J. Invest. Dermatol.* **127,** 782–791
18. Stuart, R. O., and Nigam, S. K. (1995) *Proc. Natl. Acad. Sci. U.S.A.* **92,** 6072–6076
19. Suzuki, T., Elias, B. C., Seth, A., Shen, L., Turner, J. R., Giorgianni, F., Desiderio, D., Guntaka, R., and Rao, R. (2009) *Proc. Natl. Acad. Sci. U.S.A.* **106,** 61–66
20. Abbott, N. J., Rönnbäck, L., and Hansson, E. (2006) *Nat. Rev. Neurosci.* **7,** 41–53
21. Nakagawa, S., Deli, M. A., Nakao, S., Honda, M., Hayashi, K., Nakaoke, R., Kataoka, Y., and Niwa, M. (2007) *Cell Mol. Neurobiol.* **27,** 687–694
22. Li, Y., Chen, J., Lu, W., McCormick, L. M., Wang, J., and Bu, G. (2005) *J. Cell Sci.* **118,** 5305–5314
23. Warshawsky, I., Bu, G., and Schwartz, A. L. (1993) *J. Clin. Invest.* **92,** 937–944
24. Hamanaka, H., Katoh-Fukui, Y., Suzuki, K., Kobayashi, M., Suzuki, R., Motegi, Y., Nakahara, Y., Takeshita, A., Kawai, M., Ishiguro, K., Yokoyama, M., and Fujita, S. C. (2000) *Hum. Mol. Genet* **9,** 353–361
25. Michikawa, M., Gong, J. S., Fan, Q. W., Sawamura, N., and Yanagisawa, K. (2001) *J. Neurosci.* **21,** 7226–7235
26. Elias, B. C., Suzuki, T., Seth, A., Giorgianni, F., Kale, G., Shen, L., Turner, J. R., Naren, A., Desiderio, D. M., and Rao, R. (2009) *J. Biol. Chem.* **284,** 1559–1569
27. Redig, A. J., Sassano, A., Majchrzak-Kita, B., Katsoulidis, E., Liu, H., Altman, J. K., Fish, E. N., Wickrema, A., and Platanias, L. C. (2009) *J. Biol. Chem.* **284,** 10301–10314
28. Brown, M. S., and Goldstein, J. L. (1976) *Science* **191,** 150–154
29. Bu, G., and Marzolo, M. P. (2000) *Trends Cardiovasc. Med.* **10,** 148–155
30. Bu, G., Geuze, H. J., Strous, G. J., and Schwartz, A. L. (1995) *EMBO J.* **14,** 2269–2280
31. Iadonato, S. P., Bu, G., Maksymovitch, E. A., and Schwartz, A. L. (1993) *Biochem. J.* **296,** 867–875
32. Kanekiyo, T., and Bu, G. (2009) *J. Biol. Chem.* **284,** 33352–33359
33. Ruiz, J., Kouiavskaia, D., Migliorini, M., Robinson, S., Saenko, E. L., Gorlatova, N., Li, D., Lawrence, D., Hyman, B. T., Weisgraber, K. H., and Strickland, D. K. (2005) *J. Lipid Res.* **46,** 1721–1731
34. Liu, Q., Trotter, J., Zhang, J., Peters, M. M., Cheng, H., Bao, J., Han, X., Weeber, E. J., and Bu, G. (2010) *J. Neurosci.* **30,** 17068–17078
35. Hara, M., Matsushima, T., Satoh, H., Iso-o, N., Noto, H., Togo, M., Kimura, S., Hashimoto, Y., and Tsukamoto, K. (2003) *Arterioscler. Thromb. Vasc. Biol.* **23,** 269–274
36. Michikawa, M., Fan, Q. W., Isobe, I., and Yanagisawa, K. (2000) *J. Neurochem.* **74,** 1008–1016
37. Gong, J. S., Kobayashi, M., Hayashi, H., Zou, K., Sawamura, N., Fujita, S. C., Yanagisawa, K., and Michikawa, M. (2002) *J. Biol. Chem.* **277,** 29919–29926
38. Minagawa, H., Gong, J. S., Jung, C. G., Watanabe, A., Lund-Katz, S., Phillips, M. C., Saito, H., and Michikawa, M. (2009) *J. Neurosci. Res.* **87,** 2498–2508
39. Minagawa, H., Watanabe, A., Akatsu, H., Adachi, K., Ohtsuka, C., Terayama, Y., Hosono, T., Takahashi, S., Wakita, H., Jung, C. G., Komano, H., and Michikawa, M. (2010) *J. Biol. Chem.* **285,** 38382–38388
40. Steinberg, S. F. (2008) *Physiol. Rev.* **88,** 1341–1378
41. Hayashi, H., Campenot, R. B., Vance, D. E., and Vance, J. E. (2009) *J. Biol. Chem.* **284,** 29605–29613
42. Bales, K. R., Liu, F., Wu, S., Lin, S., Koger, D., DeLong, C., Hansen, J. C., Sullivan, P. M., and Paul, S. M. (2009) *J. Neurosci.* **29,** 6771–6779
43. Buttini, M., Yu, G. Q., Shockley, K., Huang, Y., Jones, B., Masliah, E., Mallory, M., Yeo, T., Longo, F. M., and Mucke, L. (2002) *J. Neurosci.* **22,** 10539–10548
44. Dolev, I., and Michaelson, D. M. (2004) *Proc. Natl. Acad. Sci. U.S.A.* **101,** 13909–13914
45. Fagan, A. M., Watson, M., Parsadanian, M., Bales, K. R., Paul, S. M., and Holtzman, D. M. (2002) *Neurobiol. Dis.* **9,** 305–318
46. Holtzman, D. M., Bales, K. R., Tenkova, T., Fagan, A. M., Parsadanian, M., Sartorius, L. J., Mackey, B., Olney, J., McKeel, D., Wozniak, D., and Paul, S. M. (2000) *Proc. Natl. Acad. Sci. U.S.A.* **97,** 2892–2897
47. He, X., Cooley, K., Chung, C. H., Dashti, N., and Tang, J. (2007) *J. Neurosci.* **27,** 4052–4060
48. Ye, S., Huang, Y., Müllendorff, K., Dong, L., Giedt, G., Meng, E. C., Cohen, F. E., Kuntz, I. D., Weisgraber, K. H., and Mahley, R. W. (2005) *Proc. Natl. Acad. Sci. U.S.A.* **102,** 18700–18705
49. Jiang, Q., Lee, C. Y., Mandrekar, S., Wilkinson, B., Cramer, P., Zelcer, N., Mann, K., Lamb, B., Willson, T. M., Collins, J. L., Richardson, J. C., Smith, J. D., Comery, T. A., Riddell, D., Holtzman, D. M., Tontonoz, P., and Landreth, G. E. (2008) *Neuron* **58,** 681–693
50. Bell, R. D., Deane, R., Chow, N., Long, X., Sagare, A., Singh, I., Streb, J. W., Guo, H., Rubio, A., Van Nostrand, W., Miano, J. M., and Zlokovic, B. V. (2009) *Nat. Cell Biol.* **11,** 143–153
51. Ito, S., Ohtsuki, S., Kamiie, J., Nezu, Y., and Terasaki, T. (2007) *J. Neurochem.* **103,** 2482–2490
52. Zlokovic, B. V. (2008) *Neuron* **57,** 178–201
53. Deane, R., Sagare, A., Hamm, K., Parisi, M., Lane, S., Finn, M. B., Holtzman, D. M., and Zlokovic, B. V. (2008) *J. Clin. Invest.* **118,** 4002–4013
54. Dickstein, D. L., Biron, K. E., Ujiie, M., Pfeifer, C. G., Jeffries, A. R., and Jefferies, W. A. (2006) *FASEB J.* **20,** 426–433
55. Ujiie, M., Dickstein, D. L., Carlow, D. A., and Jefferies, W. A. (2003) *Microcirculation* **10,** 463–470
56. Nagababu, E., Usatyuk, P. V., Enika, D., Natarajan, V., and Rifkind, J. M. (2009) *J. Alzheimers Dis.* **17,** 845–854
57. Bell, R. D., Winkler, E. A., Sagare, A. P., Singh, I., LaRue, B., Deane, R., and Zlokovic, B. V. (2010) *Neuron* **68,** 409–427

THE JOURNAL OF BIOLOGICAL CHEMISTRY VOL. 286, NO. 8, pp. 6393–6401, February 25, 2011

Lipoprotein Lipase Is a Novel Amyloid β (Aβ)-binding Protein That Promotes Glycosaminoglycan-dependent Cellular Uptake of Aβ in Astrocytes*[S]

Received for publication, August 4, 2010, and in revised form, November 23, 2010 Published, JBC Papers in Press, December 21, 2010, DOI 10.1074/jbc.M110.172106

Kazuchika Nishitsuji[‡], Takashi Hosono[‡], Kenji Uchimura[‡§], and Makoto Michikawa[‡1]

From the [§]Section of Pathophysiology and Neurobiology, [‡]Department of Alzheimer's Disease Research, National Center for Geriatrics and Gerontology, Obu, Aichi 474-8511, Japan

Lipoprotein lipase (LPL) is a member of a lipase family known to hydrolyze triglyceride molecules in plasma lipoprotein particles. LPL also plays a role in the binding of lipoprotein particles to cell-surface molecules, including sulfated glycosaminoglycans (GAGs). LPL is predominantly expressed in adipose and muscle but is also highly expressed in the brain where its specific roles are unknown. It has been shown that LPL is colocalized with senile plaques in Alzheimer disease (AD) brains, and its mutations are associated with the severity of AD pathophysiological features. In this study, we identified a novel function of LPL; that is, LPL binds to amyloid β protein (Aβ) and promotes cell-surface association and uptake of Aβ in mouse primary astrocytes. The internalized Aβ was degraded within 12 h, mainly in a lysosomal pathway. We also found that sulfated GAGs were involved in the LPL-mediated cellular uptake of Aβ. Apolipoprotein E was dispensable in the LPL-mediated uptake of Aβ. Our findings indicate that LPL is a novel Aβ-binding protein promoting cellular uptake and subsequent degradation of Aβ.

Lipoprotein lipase (LPL)[2] catalyzes the hydrolysis of triacylglycerol and mediates the cellular uptake of lipoproteins by functioning as a "bridging molecule" between lipoproteins and sulfated glycosaminoglycans (GAGs) or lipoprotein receptors in blood vessels (1, 2). Sulfated GAGs are side chains of proteoglycans normally found in the extracellular matrix and on the cell surface in the peripheral tissues and brain. Sulfation modifications vary within the GAG chains and are crucial for interaction between GAGs and various protein ligands (3), including LPL (4, 5).

It has been shown that LPL is distributed in numerous organs and is highly expressed in the brain (6, 7). Although the catabolic activity of LPL on triacylglycerol is observed in the brain (8), the finding that apolipoprotein CII (apoCII), an essential cofactor for LPL, is not expressed in the brain (9, 10), suggests that LPL has a novel nonenzymatic function in the brain. However, little is known about LPL function in the brain. Interestingly, it has been shown that LPL is accumulated in senile plaques of Alzheimer disease (AD) brains (11). Moreover, SNPs in the coding region of the LPL gene are associated with disease incidence in clinically diagnosed AD subjects, LPL mRNA expression level, brain cholesterol level, and the severity of AD pathologies, including neurofibrillary tangles and senile plaque density (12). These results suggest that LPL may have a physiological role in the brain, whose alternation is associated with the pathogenesis of AD.

The occurrence of senile plaques in the brain is one of the pathological hallmarks of AD. They contain extracellular deposits of amyloid β protein (Aβ), and the abnormal Aβ deposition or the formation of soluble Aβ oligomers is crucial for AD pathogenesis. Aβ is a physiological peptide whose main species are 40 and 42 amino acids in length, and Aβ42 is the predominant specie in senile plaques (13). The Aβ levels are determined by the balance between its production and degradation/clearance, and an attenuated Aβ catabolism is suggested to cause Aβ accumulation in aging brains (14). Previous studies have shown that astrocytes and microglia directly take up and degrade Aβ42 (15, 16) and that Aβ degradation occurs in late endosomal-lysosomal compartments (17, 18). These lines of evidence, together with the finding that LPL mediates the cellular uptake of lipoproteins (1, 2), led us to carry out experiments to determine whether LPL interacts with Aβ to promote Aβ cellular uptake and degradation in astrocytes. Here, we provide evidence that LPL forms a complex with Aβ and facilitates Aβ cell surface binding and uptake in mouse primary astrocytes through a mechanism that is dependent on heparan sulfate and chondroitin sulfate GAG chains, leading to the lysosomal degradation of Aβ.

MATERIALS AND METHODS

Materials—Bovine LPL, heparinases, and a polyclonal anti-actin antibody were purchased from Sigma. Synthetic Aβ1–42 was purchased from the Peptide Institute (Osaka,

* This work was supported by a grant-in-aid for scientific research on priority areas (Research on Pathomechanisms of Brain Disorders) from the Ministry of Education, Culture, Sports, Science, and Technology of Japan, a grant from the Program for Promotion of Fundamental Studies in Health Sciences of the National Institute of Biomedical Innovation, a grant from the Ministry of Health, Labor, and Welfare of Japan (Research on Dementia, Health, and Labor Sciences Research Grant H20-007), and a grant from the Japan Health Sciences Foundation (Research on Publicly Essential Drugs and Medical Devices).

[S] The on-line version of this article (available at http://www.jbc.org) contains supplemental "Methods" and Fig. 1.

[1] To whom correspondence should be addressed: Department of Alzheimer's Disease Research, National Center for Geriatrics and Gerontology, Gengo 35, Morioka, Obu, Aichi 474-8511, Japan. Tel.: 81-562-46-2311; Fax: 81-562-46-8569; E-mail: michi@ncgg.go.jp.

[2] The abbreviations used are: LPL, lipoprotein lipase; Aβ, amyloid β; ApoE, apolipoprotein E; CS, chondroitin sulfate(s); HS, heparan sulfate; GAG, glycosaminoglycan; ANOVA, one-way analysis of variance.

Japan). Heparin, chondroitin, chondroitin sulfates, and chondroitinase ABC were from Seikagaku (Tokyo, Japan). Monoclonal anti-Aβ antibodies (6E10, 4G8) were purchased from Signet Laboratories (Dedham, MA), and a goat polyclonal anti-ApoE antibody and mouse control IgG were from Millipore (Bedford, MA). An anti-LPL antibody and Cy3- and FITC- conjugated secondary antibodies were purchased from Abcam, Inc. (Cambridge, MA). A monoclonal anti-Aβ antibody (2C8) was purchased from Medical and Biological Laboratories (Nagoya, Japan).

Animals—C57BL/6 mice were purchased from SLC, Inc. (Hamamatsu, Japan). ApoE-KO mice were obtained from Jackson ImmunoResearch Laboratories (Bar Harbor, ME). The National Center of Geriatrics and Gerontology Institutional Animal Care and Use Committee approved the animal studies.

Preparation of LPL—Because the sequence of LPL is highly conserved among mammalian species and the ability of LPL to interact with proteoglycans is also well conserved, we used LPL purified from bovine milk. An LPL suspension (suspended in 3.8 M ammonium sulfate, 0.02 M Tris-HCl, pH 8.0) was centrifuged (10,000 × *g* for 20 min at 4 °C), and the resulting pellet was dissolved in PBS. The prepared LPL was stored at 4 °C and used within 3 days.

Cell Culture—Highly astrocyte-rich cultures were prepared according to a method described previously (19). In brief, brains of postnatal day 2 C57BL/6 mice or ApoE knock-out mice were removed under anesthesia. The cerebral cortices from the mouse brains were dissected, freed from meninges, and diced into small pieces; the cortical fragments were incubated in 0.25% trypsin and 20 mg/ml DNase I in PBS at 37 °C for 20 min. The fragments were then dissociated into single cells by pipetting. The dissociated cells were seeded in 75-cm^2 dishes at a density of 5×10^7 cells per flask in DMEM-containing 10% FBS. After 10 days of incubation *in vitro*, flasks were shaken at 37 °C overnight, and the remaining astrocytes in the monolayer were trypsinized (0.1%) and reseeded. The astrocyte-rich cultures were maintained in DMEM-containing 10% FBS until use.

Assay of Aβ Binding and Uptake in Astrocytes by Western Blotting—Assays were carried out on confluent monolayers of astrocytes grown in 12-well plates. Aβ was dissolved in dimethyl sulfoxide to a final concentration of 1 mM and stored at −40 °C. Aβ (500 nM) and LPL (1–10 μg/ml) were mixed in DMEM. Immediately, the mixture was added to the culture medium of astrocytes. Cells were incubated at 37 °C for 5 h to assess the cellular uptake of Aβ or at 4 °C for 3 h to evaluate the binding of Aβ to the cell surface of astrocytes. In these assays, cells were incubated in serum-free DMEM. After incubation, cells were washed with PBS three times, harvested using a cell scraper and lysed by sonication in radioimmune precipitation assay buffer (1% Nonidet P-40, 0.5% sodium deoxycholate, 0.1% SDS, 150 mM NaCl, 50 mM Tris-HCl (pH 8.0), 1 mM EDTA). Cell lysates were subjected to SDS-PAGE with 4–20% gradient gels (WAKO Pure Chemicals, Osaka, Japan) and transferred to polyvinylidene difluoride membranes (Millipore). Aβ was probed with 6E10 antibody followed by horseradish peroxidase-labeled anti-mouse antibody (Cell Signaling Technology, Inc., Beverly, MA) and chemiluminescent substrate ECL Plus (GE Healthcare). The protein contents of cell lysates were normalized to the expression level of actin protein. To examine the involvement of GAGs, heparin, chemically modified heparins, chondroitin, or chondroitin sulfates (3 μg/ml) were incubated with a mixture solution of Aβ and LPL. Astrocytes were pretreated with a mixture of heparinase II and heparinase III or chondroitinase ABC (0.03 units/ml) for 24 h at 37 °C to evaluate endogenously expressed glycosaminoglycans. Signals were visualized and quantified using a LAS-3000 luminescent image analyzer (Fujifilm, Tokyo, Japan) and ImageJ software (National Institutes of Health, Bethesda, MD). For analyzing protein band densities, a region of interest was drawn around a band, and protein band densities were calculated.

siRNA Interference of LPL—siRNA specific for mouse LPL (sense strand, 5′-CAGCUGAGGACACUUGUCAUCUCAUdTdT-3′; antisense strand, 5′-AUGAGAUGACAAGUGUCCUCAGCUGdTdT-3′) and control siRNA (sense strand, 5′-CAGAGGGCACAUUUGACCUUUCCAUdTdT-3′; antisense strand, 5′-AUGGAAAGGUCAAAUGUGCCCUCUG-3′) was purchased from Invitrogen. Astrocytes grown in 12-well plates for 24 h were transfected with either LPL siRNA or control siRNA with Lipofectamine RNAiMAX (Invitrogen). Forty-eight hours after transfection, cells were treated with Aβ (1 μM) and then incubated at 4 °C for 3 h, and cell-surface associated Aβ was analyzed as described above. An anti-LPL antibody (Gene Tex, Inc.) was used for the detection of LPL.

Assay of Aβ Degradation in Astrocytes—Astrocytes were incubated with Aβ (250 nM) and LPL (2 μg/ml) at 37 °C for 5 h. Subsequently, cells were washed with DMEM and incubated in DMEM for additional hours. Then, Aβ in cell lysates was analyzed by Western blotting as described above.

Immunoprecipitation—Aβ (500 nM) and LPL at various concentrations were incubated in DMEM at 37 °C for 3 h. LPL-Aβ complexes were immunoprecipitated with an anti-LPL antibody and magnetic protein G beads (Dynal, Hamburg, Germany). For detection of LPL-Aβ complexes in the mice brains, brain homogenates from 12-week-old C57BL/6 mice were used. In brief, anesthetized mice were perfused with PBS containing 35 μg/ml heparin for 15 min. The cerebrum was dissected out and homogenized by sonication in 4 volumes of PBS containing a protease inhibitor mixture (P8340; Sigma) and centrifuged at 1,000 × *g* for 10 min at 4 °C. The supernatants were harvested and LPL-Aβ complexes were immunoprecipitated with an anti-LPL antibody and magnetic protein G beads. The obtained precipitates were washed three times with PBS and incubated at 70 °C for 10 min in SDS sample buffer. Dissociated Aβ recovered in the supernatant was assessed by Western blotting as described above. For detection of endogenous Aβ, the supernatants were subjected to SDS-PAGE with 4–20% gradient gels and transferred to polyvinylidene difluoride membranes. The membranes were exposed to microwave irradiation for 20 s, and Aβ was probed with 4G8 antibody followed by horseradish peroxidase-labeled anti-mouse antibody and the chemiluminescent substrate ECL Plus.

Immunocytochemistry—Astrocytes grown on poly-L-lysine-coated coverslips were incubated with a mixture of Aβ (250 nM) and LPL (2 μg/ml) at 37 °C for 5 h. After treatment, the cells were fixed with 4% paraformaldehyde in PBS at room temperature for 10 min, blocked, and permeabilized with 10% normal goat serum and 0.05% saponin in PBS at room temperature for 20 min. In some experiments, cells were washed twice with DMEM followed by incubation at 37 °C for 3 h in DMEM and fixed. The cells were then incubated with primary antibodies followed by Cy3- and FITC-conjugated secondary antibodies. The stained specimens were mounted with Fluor-Save reagents (Calbiochem) and examined under an LSM 510 confocal laser microscope (Carl Zeiss MicroImaging GmbH, Jena, Germany).

Statistical Analysis—The collected data were analyzed by one-way analysis of variance (ANOVA) including appropriate variables followed by the Dunnett's test or unpaired Student's *t* test. Results were considered significant when $p < 0.05$.

RESULTS

LPL Binds to Aβ in Vitro—LPL was incubated with freshly prepared Aβ42 *in vitro*, and the complexes formed were immunoprecipitated with an anti-LPL antibody coupled with magnetic beads, followed by probing Western blots of protein complexes using an anti-Aβ antibody (Fig. 1*A*). Aβ42 was immunoprecipitated with an anti-LPL antibody, but not with control IgG. The levels of Aβ42 recovered in the immunoprecipitates from samples in the presence of 2–5 μg/ml LPL were significantly higher than those from samples in the presence of 0, 0.5, or 1 μg/ml of LPL (Fig. 1, *B* and *C*), suggesting that LPL directly interacts with Aβ42, and these two molecules form a complex in an LPL dose-dependent manner. Furthermore, endogenous mouse Aβ was immunoprecipitated with the anti-LPL antibody from brain homogenates prepared from C57BL/6 mice (Fig. 1*D*), indicating that endogenous mouse LPL directly interacts with endogenous mouse Aβ. We also determined the assembly state of Aβ that forms complex with LPL. Solutions containing Aβ oligomers were subjected to immunoprecipitation/immunoblot analysis, and Aβ42 monomers were immunoprecipitated by an anti-LPL antibody (supplemental Fig. 1).

LPL Promotes Cell Surface Binding and Cellular Uptake of Aβ in Astrocytes—We then determined whether LPL affects the cellular binding of Aβ to astrocytes. Soluble Aβ42 and various concentrations of LPL were added to primarily cultured astrocytes prepared from WT mice and then incubated at 4 °C. LPL (2–5 μg/ml) of significantly augmented Aβ42 binding to astrocytes by 5.8- to 9-fold of that in the case without LPL (Fig. 2, *A* and *B*). To examine the effect of LPL on the cellular uptake of Aβ, we incubated primary astrocytes with soluble Aβ42 at 37 °C for 5 h. Apparently, the level of Aβ uptake by astrocytes increased in the presence of LPL at concentrations of 2 to 5 μg/ml (Fig. 2*C*, lysate). Consistent with the increase in the level of cellular uptake of Aβ, the level of Aβ remaining in culture medium was decreased (Fig. 2*C*, medium). The Aβ levels in the cell lysate quantified are shown in Fig. 2*D*, indicating that Aβ levels were significantly increased by 5–8-fold that in astrocytes incubated without LPL. Next,

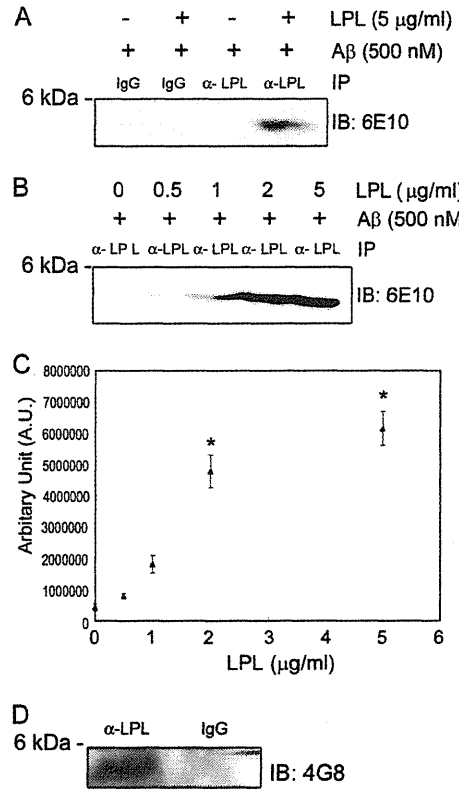

FIGURE 1. **LPL binds to Aβ *in vitro*.** *A*, LPL (5 μg/ml) and Aβ (500 nM) were incubated in DMEM at 37 °C for 3 h. Protein complexes formed were immunoprecipitated with an anti-LPL antibody (α-LPL), and the immunoprecipitates (*IP*) were analyzed by Western blotting using 6E10, an anti-Aβ antibody. These data are representative of three independent experiments. *B*, LPL at various concentrations of 0, 0.5, 1, 2, and 5 μg/ml and Aβ at 500 nM were incubated in DMEM at 37 °C for 3 h. Protein complexes formed were immunoprecipitated with an α-LPL, and the immunoprecipitates were subjected to Western blotting using 6E10. *C*, quantification of Aβ immunoprecipitated with α-LPL. The data presented are the means ± S.D. of three independent experiments. *, $p < 0.001$ *versus* samples without LPL treatment. *D*, the mouse cerebrum was homogenized by sonication in 4 volumes of PBS containing a protease inhibitor mixture and centrifuged at 1000 × *g* for 10 min at 4 °C. The supernatants were harvested. LPL-Aβ complexes in the supernatant were immunoprecipitated with an α-LPL, and the Aβ in the immunoprecipitates was detected by Western blotting using 4G8, an anti-Aβ antibody. *IB*, immunoblot.

we determined the time-dependent effect of LPL-mediated Aβ uptake into astrocytes. Astrocyte cultures were incubated with Aβ (500 nM) and LPL (2 μg/ml) at 37 °C for various hours, and the Aβ level in the cell lysate was determined. The level of Aβ in the cell lysate increased in a time-dependent manner (Fig. 2*E*). The Aβ levels in the astrocytes incubated for 3 and 5 h were significantly higher by 9–14-fold of that in astrocytes incubated without LPL (Fig. 2*F*). These concentrations of LPL are comparable with the concentrations with which LPL could act as "bridging molecules" (2, 20). There were no significant differences among the values for cultures without LPL (one-way ANOVA, $p = 0.1386$). No change in cellular morphology or cell number in astrocyte cultures was observed during the incubation (data not shown). To examine the involvement of LPL expressed by astrocytes, we carried out experiments using the gene silencing technique for LPL. The transient knockdown of LPL expression was achieved by the transfection of siRNA specific for LPL. After transfection,

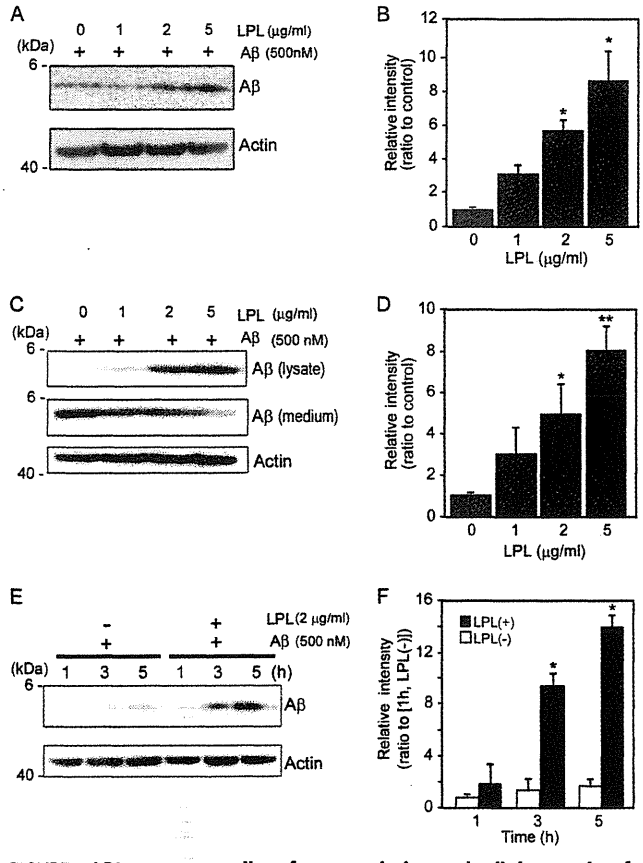

FIGURE 2. **LPL augments cell-surface association and cellular uptake of Aβ in astrocytes.** *A*, mouse primary astrocytes were incubated with LPL (0–5 μg/ml) and Aβ (500 nM) at 4 °C for 3 h. The astrocytes were washed in cold PBS three times, and the cells were harvested using a scraper. The level of Aβ on the cell surface was determined by Western blotting in a detergent extract of whole cells. *B*, quantification of cell-surface-associated Aβ. The data are the means ± S.D. of three independent experiments. *, $p < 0.001$ *versus* LPL at 0 μg/ml. *C* and *D*, astrocytes were incubated with Aβ (500 nM) and LPL (0, 1, 2, and 5 μg/ml) at 37 °C for 3 h. The cultured cells were then washed thoroughly in PBS for three times, and the cells were collected. The level of Aβ in the whole cell lysate (*lysate*), and the conditioned medium of cultured cells (*medium*) were determined by Western blotting using 6E10 antibody. The level of actin demonstrated by Western blotting using an anti-β-actin antibody was used as the loading control. These data are representative of at least three independent experiments. *D*, quantification of cellular Aβ is shown. The data presented are the means ± S.D. of three independent experiments. *, $p < 0.05$; **, $p < 0.01$ *versus* LPL at 0 μg/ml. *E* and *F*, astrocytes were incubated with Aβ (500 nM) and LPL (2 μg/ml) at 37 °C for 0, 3, and 5 h. The cultured cells were then washed thoroughly in PBS three times, and the cells were collected. The amount of Aβ in the whole cell lysate was determined by Western blotting using 6E10 antibody. The level of actin demonstrated by Western blotting using the anti-β-actin antibody was used as the loading control. These data are representative of at least three independent experiments. *F*, quantification of cellular Aβ is shown. The data are the means ± S.D. of three independent experiments. *, $p < 0.001$ *versus* LPL (+) at 1 h.

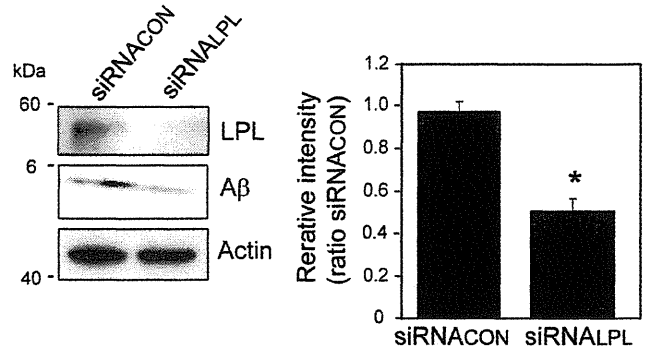

FIGURE 3. **Effect of LPL knockdown on cell-surface association of Aβ in cultured astrocytes.** Astrocytes were transfected with 10 nM siRNA specific for LPL (*siRNALPL*) and control siRNA (*siRNACON*). Forty-eight hours after transfection, cells were treated with Aβ42 (1 μM) at 4 °C for 3 h. The cells were washed in cold PBS three times, and the cells were harvested using a scraper. The level of Aβ42 on the cell surface was determined by Western blotting in a detergent extract of whole cells. The graph shows the levels of cell-surface-associated Aβ. The data are the means ± S.D. of three independent experiments. *, $p < 0.001$ *versus* control siRNA by unpaired Student's *t* test.

cells were treated with Aβ42 (1 μM) and then incubated at 4 °C for 3 h. As shown in Fig. 3, the cellular binding of Aβ42 to astrocytes was significantly decreased by LPL protein knockdown.

Degradation of Internalized Aβ in a Lysosomal Pathway in Astrocytes—Next, we examined the degradation of internalized Aβ. Mouse primary astrocytes were incubated with soluble Aβ42 and LPL at 37 °C for 5 h, washed in DMEM three times, and cultured at 37 °C for additional time (0, 3, 5, 12, and 24 h). Cells were then harvested, and the Aβ level in the cell lysate was analyzed by Western blotting. The strong signal representing internalized Aβ during the initial incubation for 5 h was detected in the cell lysate at the point of 0 min after washing (Fig. 4*A*). Three to five hours after washing, the level of Aβ remaining in the cell lysate partially disappeared (Fig. 4*A*). Twelve and twenty-four hours after washing, the internalized Aβ completely disappeared, indicating that the internalized Aβ was degraded in astrocytes in a time-dependent manner (Fig. 4*A*). To gain insight into the degradation pathway of the internalized Aβ, we investigated the localization of Aβ by immunocytochemical analysis. Mouse primary astrocytes were plated on poly-L-lysine-coated coverglasses and incubated with Aβ42 (500 nM) and LPL (2 μg/ml) at 37 °C for 5 h. In some experiments, cells were washed in DMEM three times and further incubated in serum-free DMEM for 3 h. Cells were then permeabilized and stained with an anti-Aβ antibody, 6E10, and an anti-LAMP2 antibody, whose staining signal is considered as a marker of late endosomes/lysosomes (21). We found that some portions of anti-Aβ antibody-positive signals were co-localized with staining signals reactive to the anti-LAMP2 antibody, showing that the internalized Aβ was trafficked into late endosomal/lysosomal compartments (Fig. 4*B*). To confirm the involvement of a lysosomal pathway in the degradation of LPL-mediated internalized Aβ, we determined the effect of chloroquine on the localization of Aβ internalized in an LPL-mediated manner. Chloroquine is a weak base and is taken up by cells, which results in the neutralization of acidic organelles such as lysosomes and impairment of their functions (22, 23). Chloroquine treatment at concentrations of 25 and 50 μg/ml prevented the degradation of internalized Aβ 12 h after washing out (Fig. 4*C*). We also tested inhibitors of neprilysin, an insulin-degrading enzyme, and cathepsin B, all of which are known to degrade Aβ. These inhibitors failed to suppress the degradation of internalized Aβ in astrocytes (data not shown). Thus, Aβ internalized in an LPL-mediated manner was degraded in a lysosomal pathway in astrocytes.

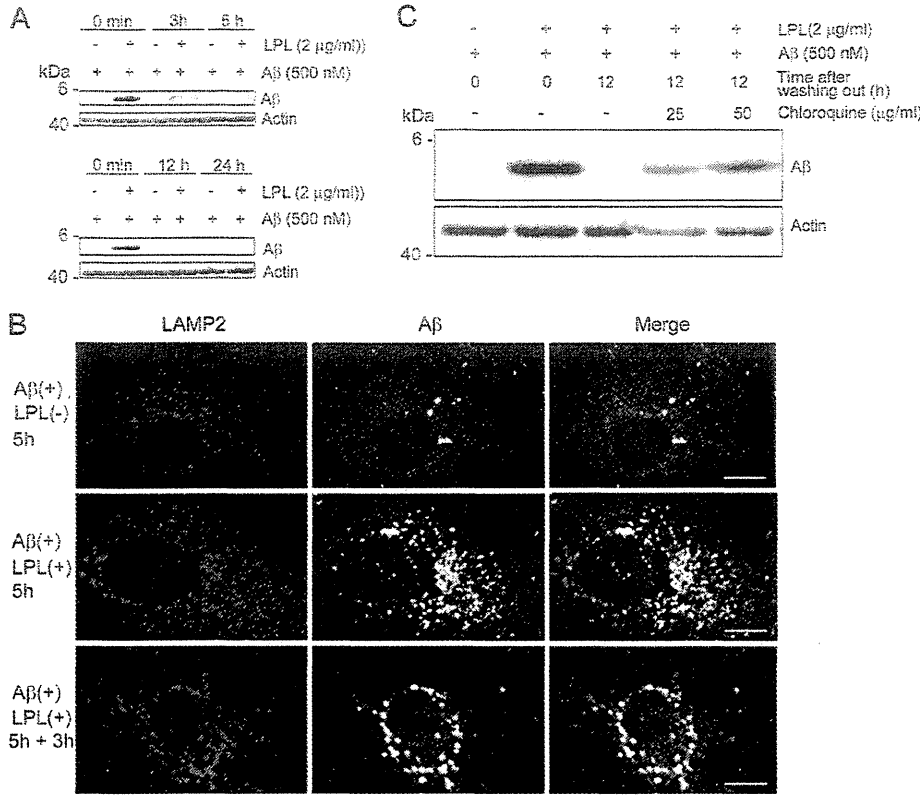

FIGURE 4. **Aβ is trafficked to late endosomal/lysosomal compartments and degraded after the LPL-mediated uptake.** *A*, mouse primary astrocytes were incubated with LPL (2 μg/ml) and Aβ (500 nM) at 37 °C for 5 h. Cells were washed in DMEM three times and then incubated in DMEM at 37 °C for 0, 3, 5, 12, and 24 h. The amount of Aβ remaining in the cells was determined by Western blotting using the anti-Aβ antibody, 6E10, in a detergent extract of whole cells. *B*, astrocytes were plated on poly-L-lysine-coated coverglasses and incubated with LPL (2 μg/ml) and Aβ (250 nM) at 37 °C for 5 h. Then, cells were permeabilized and double stained with an anti-LAMP2 antibody and 2C8. Bound antibodies were visualized with Cy3-conjugated (*red*) and FITC-conjugated (*green*) secondary antibodies for the anti-LAMP2 antibody and 6E10, respectively. Astrocytes incubated without Aβ did not show any anti-Aβ antibody-positive signals (not shown). *Scale bar*, 10 μm. *C*, astrocytes were incubated with LPL (2 μg/ml) and Aβ (500 nM) at 37 °C for 5 h. Cells were then washed in DMEM and cultured with or without chloroquine in DMEM at 37 °C for an additional 12 h. The level of Aβ in the detergent extract of whole cells was determined by Western blotting with 6E10. These are representative data of at least three independent experiments.

LPL Promotes Cellular Uptake of Aβ in a Heparan Sulfate- and Chondroitin Sulfate-dependent Manner—LPL has a high affinity with heparan sulfate (HS) and chondroitin sulfate (CS) (5, 24, 25). Therefore, we next investigated whether HS and CS are involved in the LPL-mediated cellular binding and cellular uptake of Aβ in astrocytes. Mouse primary astrocytes were pretreated with a mixture of heparinase II and heparinase III and/or chondroitinase ABC for 24 h at 37 °C, followed by incubation with Aβ42 and LPL at 4 °C for 3 h. There were no significant differences among the values in the absence of LPL (one-way ANOVA; $p = 0.0929$ for cell-surface-associated Aβ, $p = 0.4350$ for cellular Aβ). Pretreatment with heparinases or chondroitinase ABC partially decreased the level of LPL-mediated cellular binding of Aβ in astrocytes to 40 or 50% of that observed in the nontreated control, respectively (Fig. 5*A*). Interestingly, pretreatment with both heparinases and chondroitinase ABC decreased the level of LPL-mediated binding of Aβ to astrocytes to 20% of that observed in nontreated control (Fig. 5*A*). Next, we determined the effect of HS and/or CS on the LPL-mediated cellular uptake of Aβ. In conjunction with the effect of LPL on Aβ binding, heparinases and chondroitinase ABC decreased the level of LPL-mediated cellular uptake of Aβ in astrocytes to 30 and 50% of that observed in the nontreated control incubated with LPL, respectively (Fig. 5*B*). Pretreatment with both heparinases and chondroitinase ABC did not show an additive effect on the attenuation of LPL-promoted Aβ uptake (Fig. 5*B*). These findings indicate that HS and CS expressed in astrocytes are involved in the LPL-mediated association of Aβ with astrocytes and Aβ cellular uptake.

To further confirm the involvement of HS and CS in LPL-mediated Aβ uptake, we incubated astrocytes with various glycosaminoglycans. Heparin, which is a structural analog of HS, substantially suppressed the effect of LPL on Aβ uptake at a concentration of 3 μg/ml (Fig. 5*C*). The suppressive effect of heparin on LPL-mediated Aβ uptake was also observed in the presence of de-*N*-sulfated heparin, whereas either de-2-*O*-sulfated heparin or de-6-*O*-sulfated heparin had no effect on LPL-mediated Aβ uptake (Fig. 5*C*). None of these heparins interfered with the interaction between LPL and Aβ (Fig. 5*D*). In addition, 4-*O*-, 6-*O*-disulfated chondroitin sulfate (3 μg/ml) completely suppressed the promotive effect of LPL on Aβ uptake (Fig. 5*E*). 4-*O*-Sulfated chondroitin sulfate and 6-*O*-sulfated chondroitin sulfate moderately attenuated the function of LPL, whereas chondroitin (a nonsulfated form of chondroitin sulfate) and 2-*O*-, 6-*O*-disulfated chondroitin

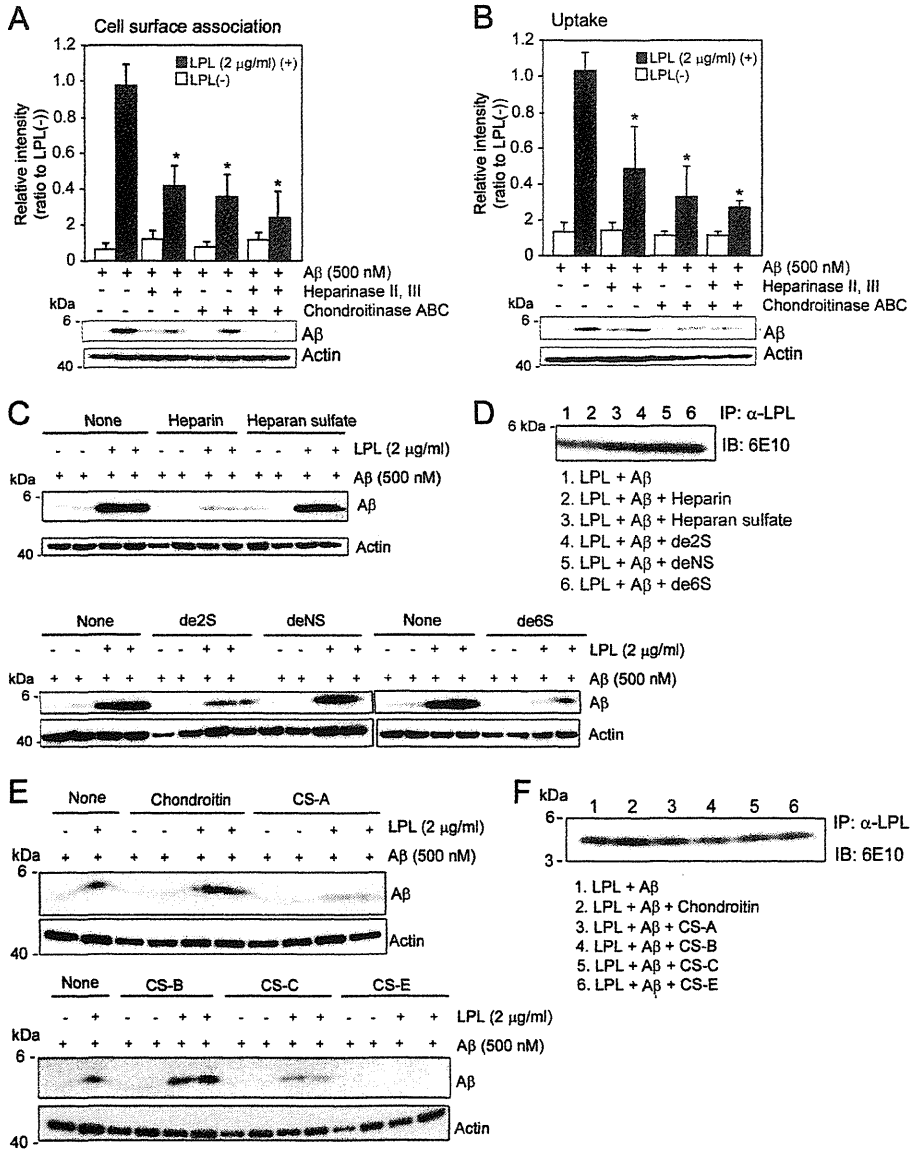

FIGURE 5. **LPL-mediated cellular binding and uptake of Aβ depends on heparan sulfate and chondroitin sulfate in astrocytes.** *A* and *B*, astrocytes from wild-type mice were pretreated with a mixture of heparinase II (0.03 μg/ml) and heparinase III (0.03 μg/ml), and/or chondroitinase ABC (0.03 μg/ml) at 37 °C for 24 h. After washing in DMEM three times, cells were incubated with LPL (2 μg/ml) and Aβ (500 nM) at 4 °C for 3 h (for cell surface association) (*A*) or 37 °C for 3 h (for uptake) (*B*). The level of Aβ in the detergent extract of whole cells was determined by Western blotting using 6E10. The quantitative assessment of cell-surface-associated Aβ (*A*) and cellular Aβ (*B*) in the present (closed bars) or absence (open bars) of LPL are shown. The data presented are the means ± S.D. of three independent experiments. * $p < 0.001$ *versus* levels of LPL (-). (*C*) Mouse primary astrocytes were incubated with Aβ (500 nM) or LPL (2 μg/ml) and Aβ (500 nM) in the presence or absence of heparin or chemically modified heparins at a concentration of 3 μg/ml at 37 °C for 5 h. The level of Aβ in the detergent extract of whole cells was determined using 6E10. (*D*) LPL (2 μg/ml) and Aβ (500 nM) were incubated in DMEM at 37 °C for 3 h in the presence or absence of heparin, heparan sulfate, or chemically modified heparins at a concentration of 3 μg/ml. Protein complexes in DMEM were immunoprecipitated (*IP*) with an anti-LPL antibody (α-LPL) and the Aβ recovered in the immunoprecipitates was analyzed by Western blotting using 6E10. These data are representative of at least three independent experiments. *de2S*, 2-*O*-desulfated heparin; *de6S*, 6-*O*-desulfated heparin; *deNS*, *N*-desulfated heparin. *E*, astrocytes were incubated with LPL (2 μg/ml) and Aβ (500 nM) in the presence or absence of chondroitin sulfates (chondroitin, chondroitin 4-sulfate (*CS-A*), 2-*O*-, 6-*O*-disulfated chondroitin sulfate (*CS-B*), 6-*O*-sulfated chondroitin sulfate (*CS-C*), and chondroitin 4,6-disulfate (*CS-E*)) at a concentration of 3 μg/ml at 37 °C for 5 h. The level of Aβ in a detergent extract of whole cells was determined by Western blotting using 6E10. *F*, LPL (2 μg/ml) and Aβ (500 nM) were incubated in DMEM at 37 °C for 3 h in the presence or absence of chondroitin sulfates at a concentration of 3 μg/ml. Protein complexes were immunoprecipitated with the anti-LPL antibody (α-LPL), and the Aβ recovered in the immunoprecipitates was analyzed by Western blotting using 6E10. The data are representative of at least three independent experiments. *IB*, immunoblot.

sulfate (also known as dermatan sulfate) did not (Fig. 5*E*). None of these CS interfered with the interaction between LPL and Aβ *in vitro* (Fig. 5*F*).

ApoE Is Dispensable for LPL-mediated Cellular Uptake of Aβ in Astrocytes—Because ApoE is reported to be involved in the metabolism of Aβ, including its aggregation and clearance (26), we analyzed the effects of ApoE on the LPL-mediated cellular uptake of Aβ in astrocytes. We collected culture media of primary astrocytes prepared from ApoE-KO mice and C57BL/6 (WT) mice. The astrocyte cultures prepared from wild-type mouse cortices were incubated in conditioned media in the presence of Aβ42 and LPL. As shown in Fig. 6A, Aβ

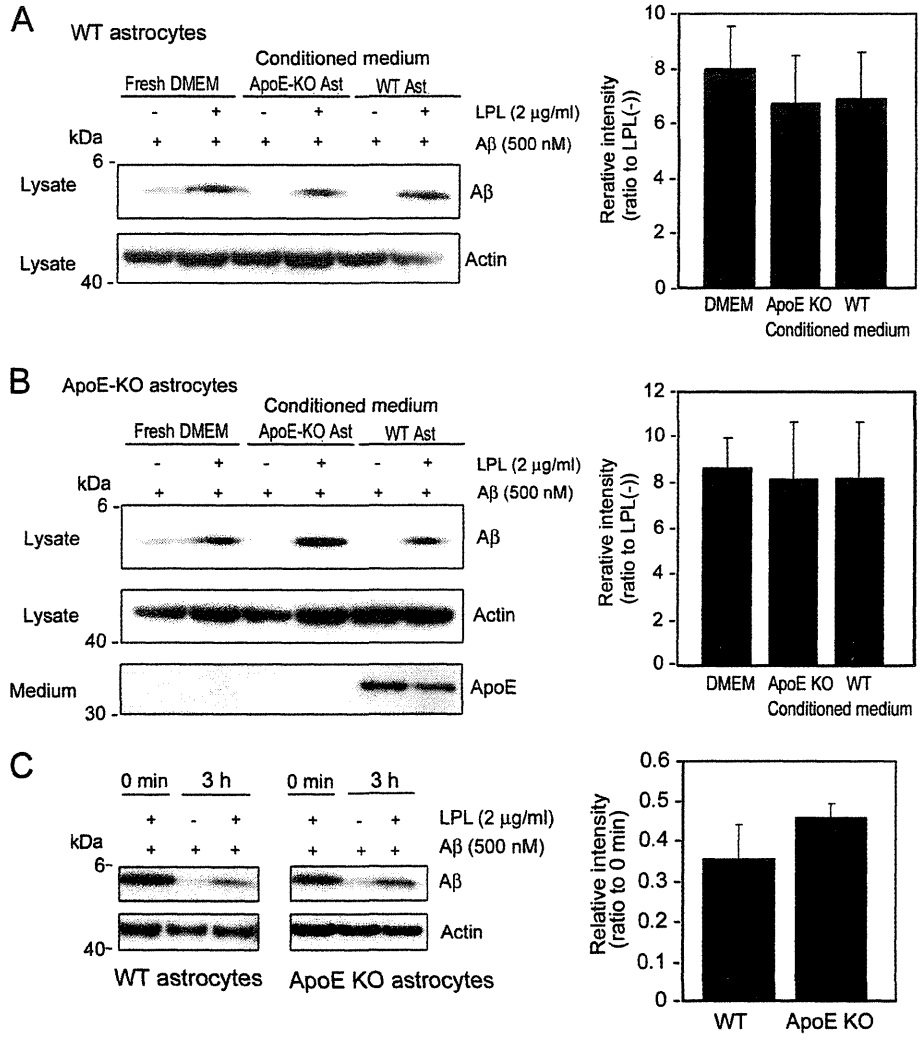

FIGURE 6. **ApoE is dispensable for the LPL-mediated cellular uptake of Aβ in astrocytes.** The astrocyte cultures prepared from WT or ApoE knock-out (KO) mice were incubated in fresh serum-free DMEM for 3 days at 37 °C. The conditioned media of these cultures were then collected. The astrocytes prepared from WT (*A*) or ApoE-KO (*B*) mouse brains were incubated in the conditioned medium of ApoE-KO astrocyte cultures or conditioned medium of WT astrocyte cultures, and LPL (2 μg/ml) and Aβ (500 nM) were added into each culture; the cultures were then maintained for another 5 h at 37 °C. After the incubation, the cultures were harvested, and the amount of cellular Aβ in a detergent extract of whole cells (*lysate*) was determined by Western blotting using 6E10. The amount of ApoE in the conditioned medium of cultured cells (*medium*) was determined by Western blotting using an anti-ApoE antibody, AB947. These data are representative of at least three independent experiments. The graphs show the cellular Aβ levels. The data are the means ± S.D. of three independent experiments. *CM*, conditioned medium; *Ast*, astrocytes. *C*, mouse primary astrocytes from WT and ApoE-KO mice were incubated with soluble Aβ42 in the presence or absence of LPL at 37 °C for 5 h, washed in DMEM three times, and further incubated at 37 °C for 3 h. Cells were then harvested, and the Aβ levels in the lysate was analyzed by Western blotting. The graph shows the cellular Aβ levels. The data are the means ± S.D. of three independent experiments.

uptake was promoted by LPL in astrocytes prepared from WT mice incubated in a fresh medium, the conditioned medium from ApoE-KO astrocytes, and the conditioned medium from WT astrocytes. There were no significant differences between these three groups (one-way ANOVA; $p = 0.6419$). This is also the case for ApoE-KO astrocytes (one-way ANOVA; $p = 0.9467$) (Fig. 6*B*). These findings indicate that ApoE is dispensable for the LPL-promoted cellular uptake of Aβ in astrocytes. We also examined the effects of ApoE on the degradation of internalized Aβ. Primary astrocytes from WT and ApoE-KO mice were incubated with soluble Aβ42 and LPL at 37 °C for 5 h, washed in DMEM three times, and further incubated at 37 °C for 3 h. Cells were then harvested, and the Aβ level in the cell lysate was analyzed by Western blotting. As shown in Fig. 6*C*, there were no significant differences between the levels of Aβ remaining in the lysate of WT astrocytes and ApoE-KO astrocytes ($p = 0.1031$).

DISCUSSION

Previous studies have shown that the mRNA expression of the LPL gene and the enzymatically active LPL are found in the brain in several mammalian species (6, 7, 27). However, considering that the main fraction of lipoproteins in the brain is HDL, which contains negligible or no triacylglycerols, and that the brain lacks an essential cofactor, apoCII, it is conceivable that LPL has a different function in the brain from that in the systemic circulation serving as an enzyme with the cofactor apoCII to catalyze the hydrolysis of triacylglycerols (28). In

the present study, we found a novel function of LPL serving as an Aβ binding molecule; that is, exogenous LPL binds to Aβ and promotes cellular binding and uptake of Aβ in astrocytes. The internalized Aβ was degraded within 12 h, mainly in a lysosomal pathway. Furthermore, we have demonstrated that HS and CS glycosaminoglycans are involved in the promotion of the LPL-mediated cellular uptake of Aβ in astrocytes.

Astrocytes are a major glial cell type in the CNS and play a crucial role in neuronal development, maintenance of synapse functions, and CNS repair after injury. Additionally, astrocytes have phagocytic and proteolytic activities (29, 30) and ingest Aβ (15, 31, 32). Our results indicate that LPL strongly enhances cellular uptake of Aβ, leading to increased degradation of Aβ in astrocytes. Previous studies have shown that SNPs in the coding region of the LPL gene are associated with AD development (33) and the severity of AD pathophysiological features (12), with the molecular mechanisms underlying this association remaining unknown. It may be possible that altered function of LPL shown in this study would result in impaired Aβ clearance and subsequent accumulation of Aβ, accelerating AD development. Because the accumulation of Aβ in the extracellular space is considered to trigger Aβ aggregation and deposition, the function of LPL to enhance Aβ binding, uptake, and degradation in astrocytes may decrease Aβ levels in the brain. However, because LPL is known to regulate the uptake and transport of vitamin E to the brain, of which deficiency results in increased Aβ accumulation and presynaptic defects accompanied by impaired learning and memory function *in vivo* (34, 35), there may be other possibilities as well, that the altered LPL function regulating vitamin E transport may enhance Aβ accumulation and impair synaptic function.

It has been suggested that lysosomal dysfunction plays a major role in Aβ accumulation, thereby causing neuronal cell death (36, 37) and that chloroquine, which disrupts lysosomal pH balance, enhances Aβ accumulation in a microglial cell line (38). Our results show that almost all of the internalized Aβ was localized in lysosomes and degraded in a time-dependent manner, and this degradation was markedly inhibited by the treatment with chloroquine, suggesting that Aβ was degraded mainly in a lysosomal pathway. These findings suggest that lysosomal pathways play a critical role in the degradation of Aβ that is internalized via a novel pathway as LPL-Aβ complexes by astrocytes.

It has been shown that LPL associates with lipoproteins and the formed LPL-bound lipoprotein complexes bind to cell-surface HS proteoglycans and CS proteoglycans (1, 5, 39), promoting the cellular uptake of lipoproteins by acting as a bridging molecule (2, 40). HS proteoglycans and CS proteoglycans are present in astrocytes (41–43). We found that pretreatment of astrocytes with a mixture of heparinases or chondroitinase ABC partially attenuated the LPL-mediated Aβ uptake, and cotreatment with heparinases and chondroitinase ABC completely suppressed the LPL-mediated cellular uptake of Aβ (Fig. 4), indicating that the LPL-mediated cellular uptake of Aβ is mediated via HS proteoglycans and CS proteoglycans. Interestingly, heparin, a highly sulfated form of HS, and 4-*O*-, 6-*O*-disulfated chondroitin sulfate, a highly sulfated CS, selectively suppressed the promotion of Aβ uptake in astrocytes. These findings suggest that LPL could act as a bridging molecule between not only cell-surface GAGs and lipoproteins but also cell-surface GAGs and Aβ and facilitate the cellular uptake of Aβ in astrocytes and that certain domains modified by multiple sulfate groups are necessary for LPL to function in astrocytes.

ApoE is one of the major apolipoproteins in the brain and plays a key role in lipid transport in the brain. ApoE affects the aggregation of Aβ *in vitro* (26). PDAPP and Tg2576 transgenic mice exhibit extensive cerebral Aβ deposition. When these transgenic mice lack the murine *apoE* gene, a significant decrease in amyloid plaque formation was observed (44, 45). Furthermore, two *in vitro* studies have demonstrated that ApoE can facilitate the cellular degradation of Aβ (16, 31). These lines of evidence suggest that ApoE affects Aβ metabolism. Thus, we examined whether ApoE could be involved in the LPL-mediated cellular uptake of Aβ. LPL promoted the cellular uptake of Aβ in wild-type and ApoE-deficient astrocytes in culture. The presence or absence of ApoE in the conditioned medium of astrocytes did not alter the levels of Aβ internalized in an LPL-mediated manner. These results suggest that ApoE is not required for the LPL-mediated cellular uptake of Aβ in astrocytes.

In this study, we demonstrated a novel LPL function; that is, LPL binds to Aβ and enhances the cellular uptake of Aβ in a sulfated glycosaminoglycan-dependent manner, and the internalized Aβ is degraded in a lysosomal pathway. Although further studies will be needed to confirm the role of LPL in the clearance of Aβ *in vivo*, our findings provide a new insight into the molecular pathogenesis of AD and a potential strategy for AD therapy.

REFERENCES

1. Williams, K. J., Fless, G. M., Petrie, K. A., Snyder, M. L., Brocia, R. W., and Swenson, T. L. (1992) *J. Biol. Chem.* **267,** 13284–13292
2. Mulder, M., Lombardi, P., Jansen, H., van Berkel, T. J., Frants, R. R., and Havekes, L. M. (1993) *J. Biol. Chem.* **268,** 9369–9375
3. Kreuger, J., Spillmann, D., Li, J. P., and Lindahl, U. (2006) *J. Cell Biol.* **174,** 323–327
4. Edwards, I. J., Goldberg, I. J., Parks, J. S., Xu, H., and Wagner, W. D. (1993) *J. Lipid Res.* **34,** 1155–1163
5. Edwards, I. J., Xu, H., Obunike, J. C., Goldberg, I. J., and Wagner, W. D. (1995) *Arterioscler. Thromb. Vasc. Biol.* **15,** 400–409
6. Goldberg, I. J., Soprano, D. R., Wyatt, M. L., Vanni, T. M., Kirchgessner, T. G., and Schotz, M. C. (1989) *J. Lipid Res.* **30,** 1569–1577
7. Yacoub, L. K., Vanni, T. M., and Goldberg, I. J. (1990) *J. Lipid Res.* **31,** 1845–1852
8. Eckel, R. H., and Robbins, R. J. (1984) *Proc. Natl. Acad. Sci. U.S.A.* **81,** 7604–7607
9. Havel, R. J., Fielding, C. J., Olivecrona, T., Shore, V. G., Fielding, P. E., and Egelrud, T. (1973) *Biochemistry* **12,** 1828–1833
10. Zannis, V. I., Cole, F. S., Jackson, C. L., Kurnit, D. M., and Karathanasis, S. K. (1985) *Biochemistry* **24,** 4450–4455
11. Rebeck, G. W., Harr, S. D., Strickland, D. K., and Hyman, B. T. (1995) *Ann. Neurol.* **37,** 211–217
12. Blain, J. F., Aumont, N., Théroux, L., Dea, D., and Poirier, J. (2006) *Eur. J. Neurosci.* **24,** 1245–1251
13. Iwatsubo, T., Odaka, A., Suzuki, N., Mizusawa, H., Nukina, N., and Ihara, Y. (1994) *Neuron* **13,** 45–53
14. Tanzi, R. E., Moir, R. D., and Wagner, S. L. (2004) *Neuron* **43,** 605–608
15. Wyss-Coray, T., Loike, J. D., Brionne, T. C., Lu, E., Anankov, R., Yan, F.,

Silverstein, S. C., and Husemann, J. (2003) *Nat. Med.* **9,** 453–457
16. Jiang, Q., Lee, C. Y., Mandrekar, S., Wilkinson, B., Cramer, P., Zelcer, N., Mann, K., Lamb, B., Willson, T. M., Collins, J. L., Richardson, J. C., Smith, J. D., Comery, T. A., Riddell, D., Holtzman, D. M., Tontonoz, P., and Landreth, G. E. (2008) *Neuron* **58,** 681–693
17. Majumdar, A., Cruz, D., Asamoah, N., Buxbaum, A., Sohar, I., Lobel, P., and Maxfield, F. R. (2007) *Mol. Biol. Cell* **18,** 1490–1496
18. Mandrekar, S., Jiang, Q., Lee, C. Y., Koenigsknecht-Talboo, J., Holtzman, D. M., and Landreth, G. E. (2009) *J. Neurosci.* **29,** 4252–4262
19. Michikawa, M., Gong, J. S., Fan, Q. W., Sawamura, N., and Yanagisawa, K. (2001) *J Neurosci.* **21,** 7226–7235
20. Fernández-Borja, M., Bellido, D., Vilella, E., Olivecrona, G., and Vilaró, S. (1996) *J. Lipid Res.* **37,** 464–481
21. Fukuda, M. (1991) *J. Biol. Chem.* **266,** 21327–21330
22. de Duve, C., de Barsy, T., Poole, B., Trouet, A., Tulkens, P., and Van Hoof, F. (1974) *Biochem. Pharmacol.* **23,** 2495–2531
23. Poole, B., and Ohkuma, S. (1981) *J. Cell Biol.* **90,** 665–669
24. Bengtsson, G., Olivecrona, T., Höök, M., Riesenfeld, J., and Lindahl, U. (1980) *Biochem. J.* **189,** 625–633
25. Pillarisetti, S., Paka, L., Sasaki, A., Vanni-Reyes, T., Yin, B., Parthasarathy, N., Wagner, W. D., and Goldberg, I. J. (1997) *J. Biol. Chem.* **272,** 15753–15759
26. Kim, J., Basak, J. M., and Holtzman, D. M. (2009) *Neuron* **63,** 287–303
27. Brecher, P., and Kuan, H. T. (1979) *J. Lipid Res.* **20,** 464–471
28. Koch, S., Donarski, N., Goetze, K., Kreckel, M., Stuerenburg, H. J., Buhmann, C., and Beisiegel, U. (2001) *J. Lipid Res.* **42,** 1143–1151
29. al-Ali, S. Y., and al-Hussain, S. M. (1996) *J. Anat.* **188,** 257–262
30. Hatten, M. E., Liem, R. K., Shelanski, M. L., and Mason, C. A. (1991) *Glia* **4,** 233–243
31. Koistinaho, M., Lin, S., Wu, X., Esterman, M., Koger, D., Hanson, J., Higgs, R., Liu, F., Malkani, S., Bales, K. R., and Paul, S. M. (2004) *Nat. Med.* **10,** 719–726
32. Matsunaga, W., Shirokawa, T., and Isobe, K. (2003) *Neurosci. Lett.* **342,** 129–131
33. Baum, L., Chen, L., Masliah, E., Chan, Y. S., Ng, H. K., and Pang, C. P. (1999) *Am. J. Med. Genet.* **88,** 136–139
34. Xian, X., Liu, T., Yu, J., Wang, Y., Miao, Y., Zhang, J., Yu, Y., Ross, C., Karasinska, J. M., Hayden, M. R., Liu, G., and Chui, D. (2009) *J. Neurosci.* **29,** 4681–4685
35. Nishida, Y., Ito, S., Ohtsuki, S., Yamamoto, N., Takahashi, T., Iwata, N., Jishage, K., Yamada, H., Sasaguri, H., Yokota, S., Piao, W., Tomimitsu, H., Saido, T. C., Yanagisawa, K., Terasaki, T., Mizusawa, H., and Yokota, T. (2009) *J. Biol. Chem.* **284,** 33400–33408
36. Bahr, B. A., and Bendiske, J. (2002) *J Neurochem.* **83,** 481–489
37. Nixon, R. A., Cataldo, A. M., and Mathews, P. M. (2000) *Neurochem. Res.* **25,** 1161–1172
38. Chu, T., Tran, T., Yang, F., Beech, W., Cole, G. M., and Frautschy, S. A. (1998) *FEBS Lett.* **436,** 439–444
39. Eisenberg, S., Sehayek, E., Olivecrona, T., and Vlodavsky, I. (1992) *J. Clin. Invest.* **90,** 2013–2021
40. Auerbach, B. J., Bisgaier, C. L., Wölle, J., and Saxena, U. (1996) *J. Biol. Chem.* **271,** 1329–1335
41. Hsueh, Y. P., and Sheng, M. (1999) *J. Neurosci.* **19,** 7415–7425
42. Laabs, T. L., Wang, H., Katagiri, Y., McCann, T., Fawcett, J. W., and Geller, H. M. (2007) *J. Neurosci.* **27,** 14494–14501
43. Tsuchida, K., Shioi, J., Yamada, S., Boghosian, G., Wu, A., Cai, H., Sugahara, K., and Robakis, N. K. (2001) *J. Biol. Chem.* **276,** 37155–37160
44. Bales, K. R., Verina, T., Dodel, R. C., Du, Y., Altstiel, L., Bender, M., Hyslop, P., Johnstone, E. M., Little, S. P., Cummins, D. J., Piccardo, P., Ghetti, B., and Paul, S. M. (1997) *Nat. Genet.* **17,** 263–264
45. Holtzman, D. M., Bales, K. R., Wu, S., Bhat, P., Parsadanian, M., Fagan, A. M., Chang, L. K., Sun, Y., and Paul, S. M. (1999) *J. Clin. Invest.* **103,** R15–R21

Jung et al. Molecular Neurodegeneration 2011, 6:47
http://www.molecularneurodegeneration.com/content/6/1/47

MOLECULAR NEURODEGENERATION

RESEARCH ARTICLE Open Access

Beta-amyloid increases the expression level of ATBF1 responsible for death in cultured cortical neurons

Cha-Gyun Jung[1*], Kyung-Ok Uhm[1], Yutaka Miura[2], Takashi Hosono[1], Hirofumi Horike[1], Kum Kum Khanna[3], Mi-Jeong Kim[1] and Makoto Michikawa[1]

Abstract

Background: Recently, several lines of evidence have shown the aberrant expression of cell-cycle-related proteins and tumor suppressor proteins in vulnerable neurons of the Alzheimer's disease (AD) brain and transgenic mouse models of AD; these proteins are associated with various paradigms of neuronal death. It has been reported that ATBF1 induces cell cycle arrest associated with neuronal differentiation in the developing rat brain, and that gene is one of the candidate tumor suppressor genes for prostate and breast cancers in whose cells overexpressed ATBF1 induces cell cycle arrest. However, the involvement of ATBF1 in AD pathogenesis is as yet unknown.

Results: We found that ATBF1 was up-regulated in the brains of 17-month-old Tg2576 mice compared with those of age-matched wild-type mice. Moreover, our *in vitro* studies showed that Aβ1-42 and DNA-damaging drugs, namely, etoposide and homocysteine, increased the expression ATBF1 level in primary rat cortical neurons, whereas the knockdown of ATBF1 in these neurons protected against neuronal death induced by Aβ1-42, etoposide, and homocysteine, indicating that ATBF1 mediates neuronal death in response to these substances. In addition, we found that ATBF1-mediated neuronal death is dependent on ataxia-telangiectasia mutated (ATM) because the blockage of ATM activity by treatment with ATM inhibitors, caffeine and KU55933, abolished ATBF1 function in neuronal death. Furthermore, Aβ1-42 phosphorylates ATM, and ATBF1 interacts with phosphorylated ATM.

Conclusions: To the best of our knowledge, this is the first report that Aβ1-42 and DNA-damaging drugs increased the ATBF1 expression level in primary rat cortical neurons; this increase, in turn, may activate ATM signaling responsible for neuronal death through the binding of ATBF1 to phosphorylated ATM. ATBF1 may therefore be a suitable target for therapeutic intervention of AD.

Background

Alzheimer's disease (AD), a progressive neurodegenerative disorder of the elderly, is associated with a chronic loss of synapses and neuronal death, and is characterized by the presence of parenchymal deposits of amyloid-β peptides (Aβ), the major protein component of senile plaques [1,2]. Accumulation of Aβ in the brain is associated with disease-causing inherited variants of the amyloid precursor protein (APP) [3], presenilin 1 (PS1) [4], presenilin 2 (PS2) [5], and apoplipoprotein E (APOE) [6] genes, and an increased extracellular Aβ level is a major cause of neuronal death in AD. In addition to genetic evidence that Aβ promotes neuronal degeneration and death *in vivo* [7,8], *in vitro* studies show that Aβ aggregates rapidly induce neuronal death by necrosis or apoptosis [9,10], and Aβ-induced neurotoxicity involves oxidative stress, inflammation, and perturbation of calcium homeostasis [1]. However, the mechanisms by which neuronal degeneration and death occur in AD and whether they are induced by Aβ are not completely understood.

One focus in the mechanism of neuronal death in AD is the aberrant expression of cell-cycle-related proteins, such as cdc2, cdk4, cyclin B1, and cyclin D, which mediate cell cycle progression, in vulnerable neurons of the

* Correspondence: jung@ncgg.go.jp
[1]Department of Alzheimer's Disease Research, Research Institute, National Center for Geriatrics and Gerontology (NCGG), 35, Morioka, Obu, Aichi 474-8511, Japan
Full list of author information is available at the end of the article

AD brain [11-14]; these molecules play essential roles in neuronal death associated with various paradigms of neuronal death [15]. In addition to cell cycle progression molecules, a number of cell cycle inhibitors, such as p16 and p27 [13,16], and tumor suppressor proteins such as p53 and BRCA1 [17,18] are also increased in levels in the AD brain. In addition to the human AD brain, the increased expression levels of cell-cycle-related proteins were also found in transgenic mouse models of AD [19,20]. Although it is unclear why cell-cycle-related proteins show increased in levels in the AD brain and AD mouse models, one possibility is that DNA damage induced by Aβ may increase the levels of or activate these molecules. Indeed, DNA damage was found in the AD brain, and Aβ increases Cdc25A [21], Cdk4, and p53 [22] levels in primary rat neurons resulting in neuronal death. Recently, Kruman et al. have reported that cultured postmitotic cortical neurons exposed to Aβ undergo apoptosis that is dependent on tumor suppressor factor ataxia-telangiectasia mutated (ATM) activity, whereas treatment with caffeine, which is an ATM inhibitor, can exert a neuroprotective effect on cultured neurons exposed to Aβ [22]. In this context, ATM appears to potentiate neuronal apoptosis.

AT-motif binding factor 1 (ATBF1) is a 404 kDa transcription factor that contains 4 homeodomains and 23 zinc-finger motifs [23] involved in transcription regulations and protein-protein interactions [24]. We previously reported that ATBF1 is highly expressed in postmitotic neurons but not in neural progenitor cells, and it induces cell cycle arrest associated with neuronal differentiation in the developing rat brain [25]. We also found that sublocalization of ATBF1 is regulated by phospatidylinositol-3 (PI3) kinase including ATM [25], indicating that ATBF1 is one of the targets of ATM. Indeed, ATM phosphorylates ATBF1 at Ser1180 in HEK293T cells exposed to 10-Gy radiation [26]. ATBF1 also interacts with p53 to activate the $p21^{Waf1/Cip1}$ promoter to trigger cell cycle arrest [27]. It has also been reported that the ATBF1 gene is one of the candidate tumor suppressor genes for prostate and breast cancers in whose cells overexpressed ATBF1 induces cell cycle arrest [28,29]. However, the involvement of ATBF1 in AD pathogenesis is as yet unknown.

In this study, we investigated whether ATBF1 expression is altered in the brains of Tg2576 mice similarly to other cell-cycle-related molecules, and we found an up-regulated ATBF1 expression in the brains of Tg2576 mice compared with those of age-matched wild-type mice. Moreover, our *in vitro* studies showed that Aβ and DNA-damaging drugs, namely, etoposide and homocysteine, increased the ATBF1 expression level in primary rat cortical neurons; this increase, in turn, may activate ATM signaling responsible for neuronal death through the binding of ATBF1 to phosphorylated ATM.

Results

ATBF1 was up-regulated in the brains of 17-month-old Tg2576 mice compared with those of age-matched wild-type mice

We first investigated whether ATBF1 expression is altered in the brains of Tg2576 mice overexpressing human APP with the Swedish mutation. Total proteins were extracted from whole brains of 10- and 17-month-old Tg2576 and age-matched wild-type mice, and subjected to Western blot analysis. We found that the ATBF1 expression level in the brains of 17-month-old wild-type mice was lower than that in the brains of 10-month-old wild-type mice. However, ATBF1 expression was significantly up-regulated in 17-month-old Tg2576 mice compared with age-matched wild-type mice, whereas there was no significant difference between Tg2576 and wild-type mice at the age of 10 months (Figure 1).

Aβ1-42 and DNA-damaging drugs, etoposide and homocysteine, increased ATBF1 expression level in cultured rat cortical neurons

In Tg2576 brains, the accumulation of Aβ occurs from 15 to 23 months but is not observed in appreciable amounts until 12 months [30]. Therefore, we hypothesized that an increase in ATBF1 expression level in the brains of 17-month-old Tg2576 mice is due to an increase in Aβ level. To test this hypothesis, we determined by Western blot analysis the protein expression levels of ATBF1 and p53, which play a key role in the regulation of cell viability in response to DNA-damaging drugs in many cell types including neurons, in cultured rat cortical neurons treated with 10 μM Aβ1-42 for 16 h. The Aβ1-42 peptide used in our experiments was largely monomer (see "Additional file 1"). We observed that Aβ1-42 significantly increased ATBF1 and p53 protein expression levels in these cells (Figure 2A). A previous study showed that the expression level of ATBF1 is increased in gastric cancer cells exposed to mitomycin-C, which can induce DNA damage in many cell types [31]. This finding suggests that DNA damage might increase ATBF1 expression level because Aβ can also induce neuronal apoptosis through oxidative DNA damage. Therefore, we treated cultured cortical neurons with two different DNA-damaging drugs, etoposide and homocysteine, which are used commonly as DNA-damaging drugs for many cells types including neurons, and we found that these two drugs significantly increased ATBF1 and p53 protein expression levels (Figure 2A). Next, we measured the expression levels of ATBF1 mRNA in cultured cortical neurons treated with Aβ1-42 at an indicated dose by semiquantitative real-time PCR analysis. As

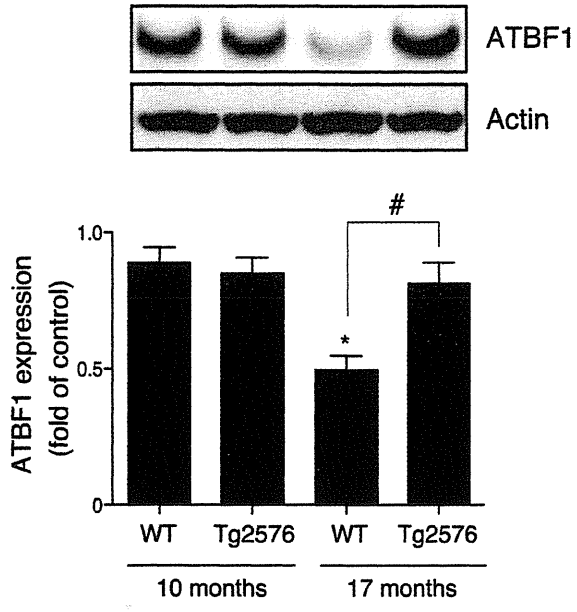

Figure 1 ATBF1 protein expression level appears to decrease in age-dependent manner in wild-type mice. It increased in the brains of 17-month-old Tg2576 mice compared with age-matched wild-type mice. Lysates were prepared from whole brains of 10- and 17-month-old Tg2576 (n = 6) and age-matched wild-type (WT) mice (n = 6). The expression level of ATBF1 was determined by Western blot analysis using the anti-ATBF1 antibody. A, representative immunoblot is shown (upper panel), and bands were quantified by densitometry, normalized to actin, and expressed as a value relative to that in the 10-month-old WT mice as a control (lower graph). All the values are presented as mean ± SEM. *$p < 0.05$ *vs* 10-month-old WT mice (n = 6) and #$p < 0.05$ compared with those of 17-month-old WT mice, as determined by one-way ANOVA followed by Duncan's test.

shown in Figure 2B, treatment with Aβ1-42 significantly increased ATBF1 mRNA expression level in a dose-dependent manner compared with the control, and etoposide and homocysteine also increased ATBF1 mRNA expression level (Figure 2C). These findings indicate that an increase in ATBF1 protein expression level induced by Aβ1-42, etoposide, and homocysteine is caused by an increase in ATBF1 gene expression level.

Knockdown of ATBF1 in cultured cortical neurons protected against Aβ1-42-, etoposide-, and homocysteine-induced neurotoxicity

Aβ1-42, etoposide, and homocysteine induce death of cultured cortical neurons *in vitro* [22]. Next, we examined whether ATBF1 mediates neuronal death after treatment with Aβ1-42, etoposide, and homocysteine. For this purpose, we first decreased the ATBF1 expression level in primary cortical neurons by ATBF1 siRNA transfection. The cells were transfected with ATBF1 siRNA-1 or control siRNA, as described in "Experimental Procedures". Forty-eight hours after transfection, the ATBF1 protein expression level was determined by Western blot analysis using an anti-ATBF1 antibody. As shown in Figures 3A and 3C, the transfection of ATBF1 siRNA-1 decreased the ATBF1 protein level by about 75% in cultured cortical neurons compared with control siRNA transfection. This finding indicates that endogenous ATBF1 can be efficiently knocked down in these cells by transfection of ATBF1 siRNA-1. Next, we determined the effects of ATBF1 knockdown on neuronal survival against Aβ1-42-, etoposide-, and homocysteine-induced neurotoxicity. Cultured cortical neurons transfected with ATBF1 siRNA-1 or control siRNA were treated with Aβ1-42 at an indicated dose, 1 μM etoposide, or 250 μM homocysteine for 16 h. Cell viability was then assessed using a CellTitle-Glo luminescent cell viability assay kit. We were able to detect differences in cell viability only by ATBF1 siRNA-1 transfection compared with control siRNA transfection. The percentage of surviving neurons decreased in control-siRNA-transfected cells after the treatment with Aβ1-42, etoposide, or homocysteine. However, the percentage of surviving neurons increased in ATBF1-siRNA-1-transfected cells compared with control-siRNA-transfected cells after the treatment with Aβ1-42 (Figure 3B), etoposide, or homocysteine (Figure 3D). These findings indicate that ATBF1 could mediate neuronal death in response to the treatment with Aβ1-42, etoposide, or homocysteine. We also determined the effects of another ATBF1 siRNA (ATBF1-siRNA-2) on neuronal survival against Aβ1-42-induced neurotoxicity, and obtained similar result (Additional file 2). Therefore, we used ATBF1 siRNA-1 to ATBF1 knockdown for the following experiments.

ATBF1 mediated apoptotic function in cultured cortical neurons against Aβ1-42-induced neurotoxicity

To determine whether apoptosis is responsible for the survival of cultured cortical neurons with decreased ATBF1 expression levels, we analyzed DNA breaks by terminal deoxynucleotidyl transferase-mediated dUTP nick-end labeling (TUNEL) assay of ATBF1-siRNA- and control-siRNA-transfected cells after Aβ1-42 treatment. Figure 4A shows representative images of TUNEL-positive cells and total nuclei. The treatment of control siRNA-transfected cells with Aβ1-42 resulted in a significant increase in the number of TUNEL-positive cells compared with nontreatment (Figure 4A). However, the percentage of TUNEL-positive cells among ATBF1-siRNA-transfected cells treated with Aβ1-42 was lower than that among control-siRNA-transfected cells (Figure 4A), indicating that the knockdown of ATBF1 significantly reduced the extent of Aβ1-42-induced apoptosis.

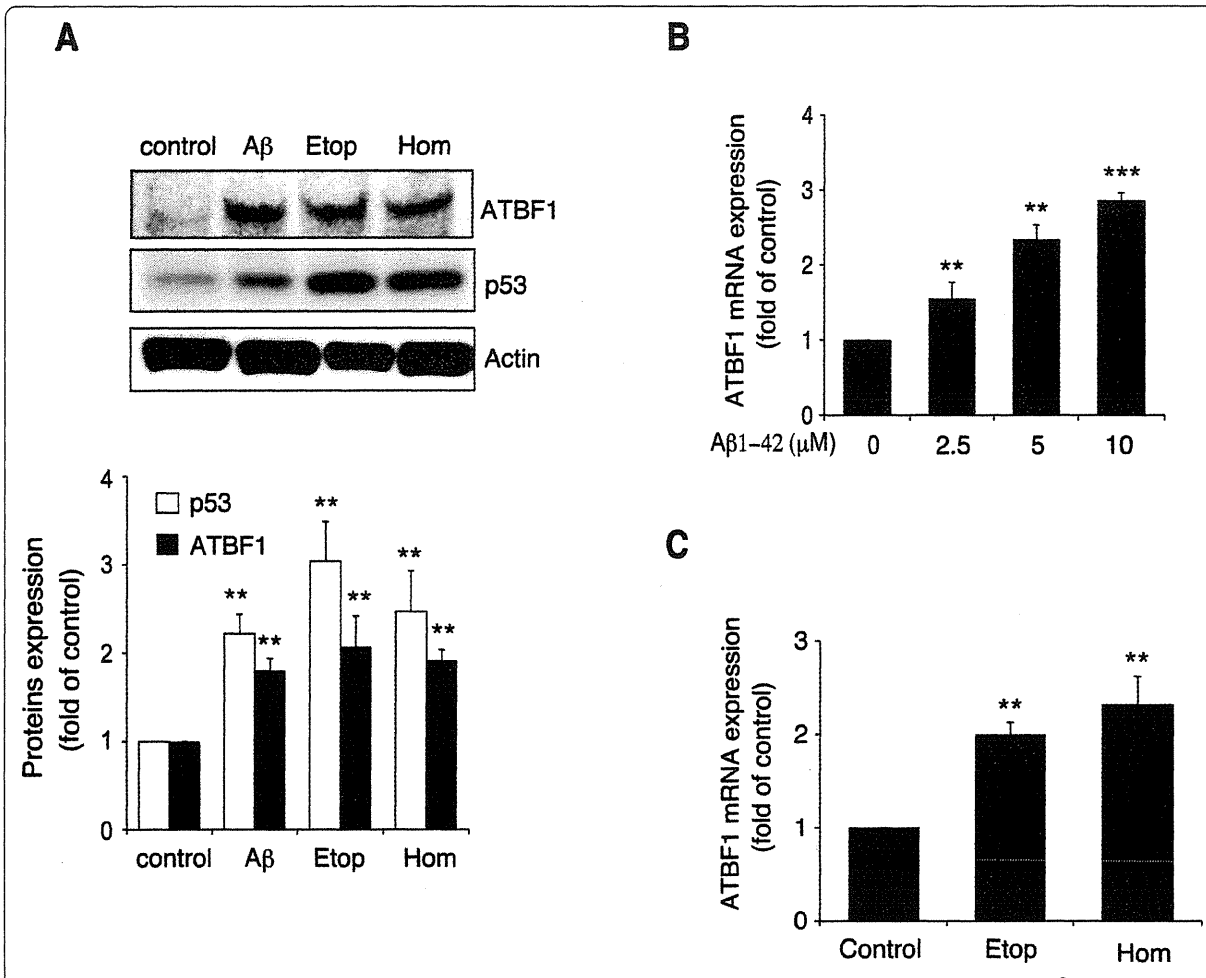

Figure 2 ATBF1 protein and mRNA expression levels increased in primary cortical neurons after treatment with Aβ1-42 and DNA-damaging drugs, namely, etoposide (Etop) and homocysteine (Hom). A, primary cortical neurons were seeded at a density of 1 × 10^6 cells/ml in poly-d-lysine-coated 60 mm culture dishes. Three days after plating, the cells were treated for 16 h with 10 μM Aβ1-42, 1 μM etoposide, or 250 μM homocysteine, and the cells were then harvested. The expression levels of ATBF1 and p53 were determined by Western blot analysis using the anti-ATBF1 and anti-p53 antibodies. A, a representative immunoblot is shown (upper panel), and bands were quantified by densitometry, normalized to actin, and expressed as a value relative to that of the control (lower panel). B and C, primary cortical neurons were treated for 16 h with 0, 2.5, 5, or 10 μM Aβ1-42 (B), or 250 μM homocysteine or 1 μM etoposide (C). ATBF mRNA expression level was determined by real-time PCR analysis. The expression level of ATBF1 mRNA was normalized to the corresponding amount of actin mRNA and expressed as a value relative to that of the control. All the values are presented as the mean ± SEM of three independent experiments. *p < 0.05, **p < 0.01, ***p < 0.001 *vs* control, as determined by Student's *t*-test.

The knockdown of ATBF1 alone showed no significant increase in the percentage of TUNEL-positive cells (Figure 4A). To confirm these findings, we performed a similar experiment, and caspase-3/7 activity was determined using a Caspase-Glo 3/7 assay kit. It has been reported that Aβ may lead to the induction of caspase-3-mediated pathways that are involved in oxidative stress [32]. The treatment of control siRNA-transfected cells with Aβ1-42 increased the activity of caspase-3/7 compared with nontreatment (Figure 4B). However, a decreased activity of caspase-3/7 was detected in ATBF1-siRNA-transfected cells treated with Aβ1-42, indicating that ATBF1 is at least one vital component for the activation of caspase-3/7 in cultured cortical neurons after Aβ1-42 treatment.

Overexpression of ATBF1 itself in primary cortical neurons did not induce apoptosis

Next, we examined whether overexpression of ATBF1 itself induces apoptosis in cultured cortical neurons. The cells were transfected with HA-tagged full-length human ATBF1 cDNA. Twenty-four hours after transfection, we performed TUNEL assay, and then counted TUNEL-positive cells among HA-ATBF1-transfected

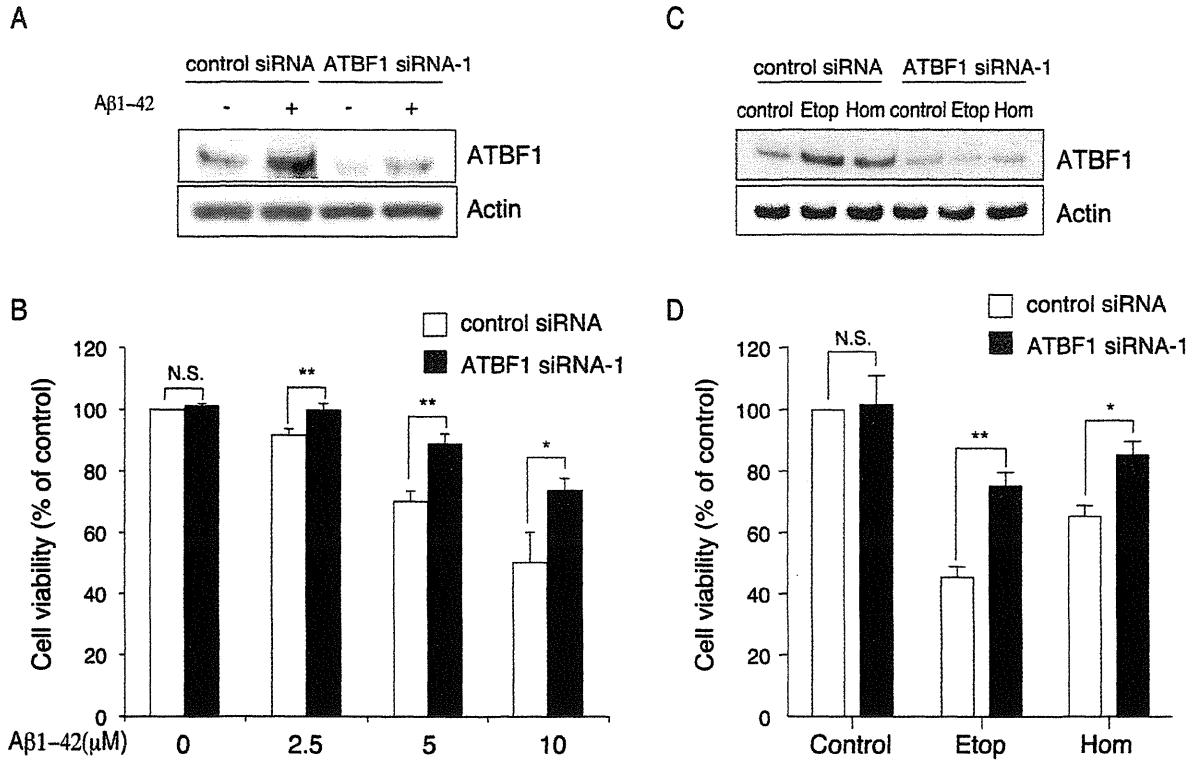

Figure 3 ATBF1 knockdown decreases the viability of primary cortical neurons upon treatment with Aβ1-42, etoposide (Etop), or homocysteine (Hom). A and C, knockdown of ATBF1 in primary cortical neurons. Primary cortical neurons were transfected with ATBF1 siRNA-1 or control siRNA for 48 h. After transfection, the cells were then incubated in the presence or absence of 10 μM Aβ1-42 (A), 1 μM etoposide (C), or 250 μM homocysteine (C) for 16 h. The expression levels of ATBF1 and actin were determined by Western blot analysis using the anti-ATBF1 and anti-actin antibodies. B and D, primary cortical neurons were seeded at a density of 1 × 10^6 cells/ml in poly-d-lysine-coated 96-well plates. Three days after plating, cells were transfected with ATBF1 siRNA-1 or control siRNA for 48 h, and the cells were then treated with 0, 2.5, 5, or 10 μM Aβ1-42 (B), 1 μM etoposide (D), or 250 μM homocysteine (D) for 16 h. Cell viability was determined using a CellTiter-Glo luminescent cell viability assay kit and is shown as a percentage of surviving cells. All the values are presented as the mean ± SEM of three independent experiments. *$p < 0.05$, **$p < 0.01$ *vs* control siRNA treatment. N.S., not significant, as determined by Student's *t*-test.

cells. We found that cells transfected with HA-ATBF1 were largely TUNEL-negative (95.2 ± 1.2%) (Figure 5). This finding is consistent with our previous finding that overexpression of ATBF1 in Neuro 2A cells (mouse neuroblastoma cell line) by transfection of the HA-ATBF1 expression vector did not induce apoptosis [25].

ATBF1-mediated neuronal death after Aβ1-42 treatment depended on ATM

Recent findings have shown that the ATM signaling pathway is essential for Aβ-induced neuronal death *in vitro* and *in vivo*, and treatment with caffeine, an inhibitor of ATM, protects cultured cortical neurons against apoptosis induced by Aβ1-42 [22]. Our previous data have shown that the nuclear localization of ATBF1 is suppressed by treatment with caffeine, indicating that ATBF1 function could be regulated by ATM [25]. Moreover, it has also been reported that the ATBF1 gene is one of the target genes of ATM, which phosphorylates ATBF1 at Ser1180 [26]. Therefore, we examined whether ATBF1-mediated neuronal death after Aβ1-42 treatment is dependent on ATM. To determine whether caffeine can protect against neuronal death induced by Aβ1-42, we analyzed the effects of caffeine on cell viability (Figure 6A) and caspase-3/7 activity (Figure 6B). Cultured cortical neurons were pretreated with 10 μM caffeine for 1 h and subsequently treated with 2.5 μM and 5 μM Aβ1-42 for 16 h. The cells were then assessed for cell viability and caspase-3/7 activity using CellTitle-Glo luminescent cell viability assay and Caspase-Glo™ 3/7 assay kits, respectively. As shown in Figures 6A and 6B, treatment with caffeine decreased the number of dead cells treated with Aβ1-42 (Figure 6A) and decreased caspase-3/7 activity (Figure 6B) compared with the nontreatment control. We also tested the effect of KU55933, a specific inhibitor of ATM [33], on cell viability. As shown in Additional file 3A, treatment with KU55933 decreased the number of

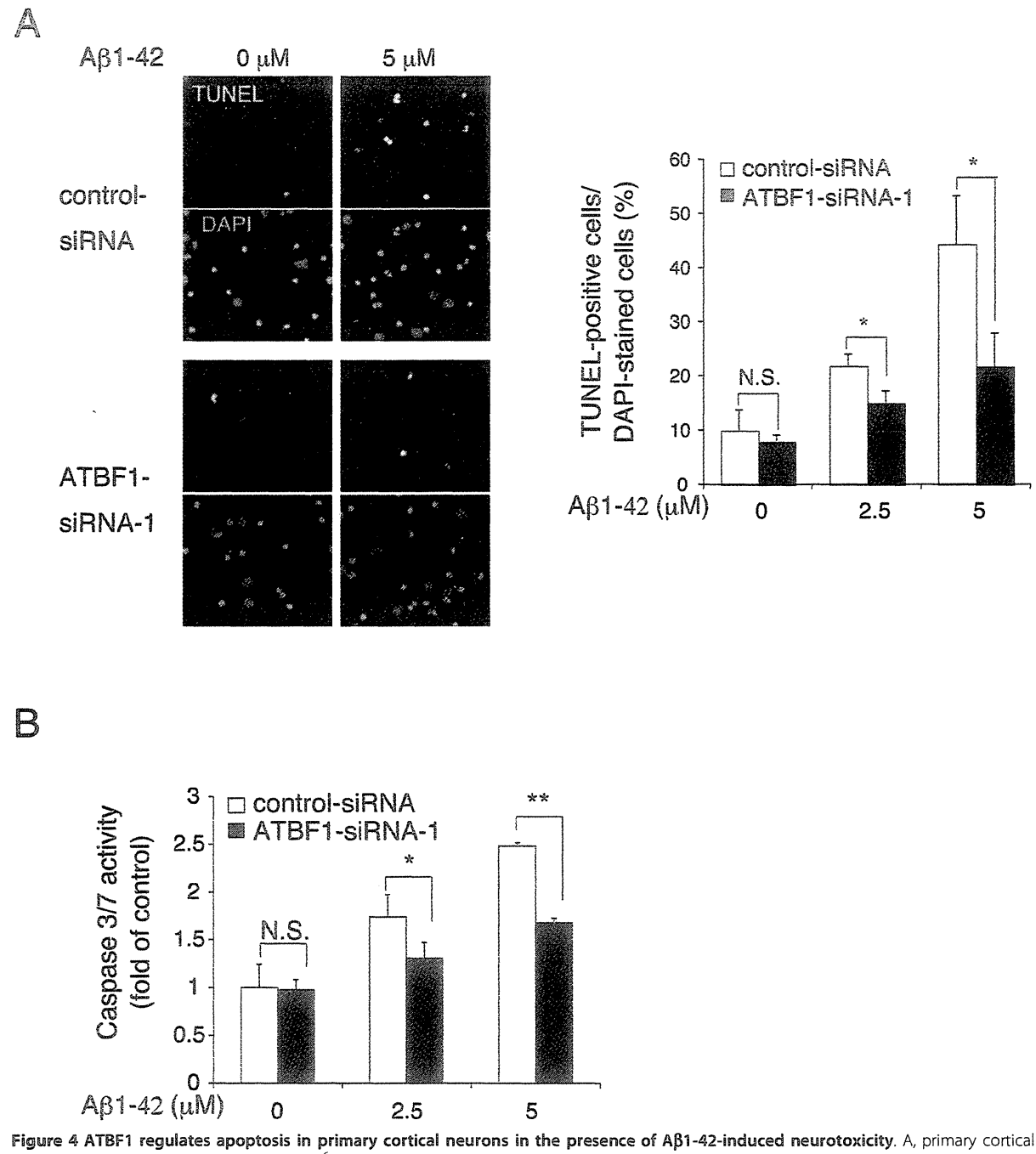

Figure 4 ATBF1 regulates apoptosis in primary cortical neurons in the presence of Aβ1-42-induced neurotoxicity. A, primary cortical neurons were seeded at a density of 1×10^6 cells/ml in poly-d-lysine-coated 24-well glass plates. Three days after plating, the cells were transfected with ATBF1 siRNA-1 or control siRNA for 48 h. After transfection, the cells were then incubated with 0, 2.5, or 10 μM Aβ1-42 for 16 h, and apoptosis was analyzed by TUNEL assay. Cell nuclei were also stained with DAPI. Left panel: Representative images showing DAPI-stained and TUNEL-positive cells. Right panel: quantification of TUNEL. TUNEL-positive neurons were counted from at least 400 neurons from five randomly selected fields in three independent experiments. B, primary cortical neurons were seeded at a density of 1×10^5 cells/ml in poly-d-lysine-coated 96-well plates. Three days after plating, cells were transfected with ATBF1 siRNA-1 or control siRNA for 48 h, and the cells were then treated with 0, 2.5, or 5 μM Aβ1-42 for 16 h. Caspase-3/7 activity was determined using a Caspase-Glo™ 3/7 assay kit. All the values are presented as the mean ± SEM of three independent experiments. $^*p < 0.05$, $^{**}p < 0.01$ *vs* control siRNA. N.S., not significant, as determined by one-way ANOVA followed by Duncan's test.